

Performance Improvement of the AOA Estimation Algorithm Using the Newton Iteration

Joon-Ho Lee and Sung-Woo Cho

Department of Information and Communication Engineering,
Sejong University, Seoul 143-747, Korea
joonhlee@sejong.ac.kr and cheage@nate.com

Abstract — In this paper, a simple numerical method based on the Newton iteration for improving the accuracy of the Conventional beam forming algorithm, the Capon beam forming algorithm, and the MUSIC algorithm for AOA (Angle-of-Arrival) estimation is presented. Based on observation, the estimates of the AOA's for a specific AOA algorithm can be obtained from the extrema of a cost function associated with the specific AOA algorithm employed. We derive explicit expressions of the iterations used for the recursive update of the estimates of the AOA's for the conventional beam forming algorithm, the Capon beam forming algorithm, and the MUSIC algorithm. The formulation is only for the update of the azimuth angle, while the extension to the update of the elevation angle and the azimuth angle can be implemented by taking into account the dependence of the array manifold on the elevation angle as well as the azimuth angle. Note that, for estimation of the azimuth, both the UCA (uniform circular array) and the ULA (uniform linear array) can be employed, and that, for simultaneous estimation of the elevation and the azimuth angle, the UCA, not the ULA, should be adopted since ULA-based algorithm cannot uniquely estimate both the azimuth and the elevation due to the ambiguity pertinent to the ULA structure. We consider the array structure of the ULA and the UCA, but it is quite straightforward to extend the proposed scheme to an arbitrary array structure by simply modifying the array vector consistently with the specific array structure.

Index Terms - AOA, accuracy improvement, conventional beam forming algorithm, Capon beam forming algorithm, MUSIC algorithm, Newton method, UCA, and ULA.

I. INTRODUCTION

Determination of the AOA (angle-of-arrival) [1-8] of signal has been of interest to the signal processing community. The application of the study ranges from military [9-13] to civilian [14-21] applications. The conventional beam forming algorithm [1], the Capon beam forming algorithm [22, 23], the MUSIC (multiple signal classification) algorithm [24], the ESPRIT (estimation of signal parameters via rotational invariance techniques) algorithm [25], and the ML (maximum likelihood) algorithm [26] have been the main algorithms for AOA estimation.

In [23], the authors showed how to apply the Newton iteration to TOA (time of arrival) estimation for performance improvement. In this paper, we propose how to improve the performance of the conventional beam forming algorithm, the Capon beam forming algorithm and the MUSIC algorithm by applying Newton iteration to the initial AOA estimates with the ULA structure and the UCA structure. Although, for ease of numerical manipulation, we adopt the ULA and the UCA structure, it is quite straightforward to apply the proposed scheme to an arbitrary array structure by simply modifying the array vector in accordance with the specific array structure employed.

The formulation for the Newton iteration is based on the cost function derived from the conventional beam forming algorithm, the Capon beam forming algorithm, and the MUSIC

algorithm, respectively. In numerical results, we demonstrate the validity of the proposed scheme in terms of the estimation accuracy and the computational complexity.

The accuracy of the AOA estimation is usually quantified via the RMS error of the estimates. Our interest in this paper is to reduce the RMS error of the estimates using numerical methods. The proposed numerical procedure does not require too much computation time, which will be quite clear in the numerical results. More specifically, we give an explicit numerical formulation for the improvement of the AOA estimation for the ULA structure and the UCA structure for three different AOA estimation algorithms. The numerical formulation is essentially Newton iteration for the recursive update of AOA angles corresponding to the local extrema of the cost function of each AOA algorithm.

In practical implementation of nonparametric spectral based AOA estimation, the output can only be evaluated at discrete angles. The estimate is determined from the angle at which the output achieves the maximum value. This estimate is called the initial estimate.

II. DATA MODEL

The signal received at each antenna element can be formulated as,

$$\begin{bmatrix} x_1(k) \\ \vdots \\ x_M(k) \end{bmatrix} = [\mathbf{a}(\theta_1) \ \cdots \ \mathbf{a}(\theta_N)] \begin{bmatrix} s_1(k) \\ \vdots \\ s_N(k) \end{bmatrix} + \begin{bmatrix} n_1(k) \\ \vdots \\ n_M(k) \end{bmatrix} \\ = \mathbf{A} \cdot \mathbf{s}(k) + \mathbf{n}(k) \quad (1)$$

where $s(k)$, $\mathbf{n}(k)$, $\mathbf{a}(\theta_i)$, and \mathbf{A} are defined as,

$s(k)$: vector of incident complex monochromatic signal at time k ;

$\mathbf{n}(k)$: noise vector at each array element m , zero mean, variance σ_n^2 ;

$\mathbf{a}(\theta_i)$: M element array steering vector for the θ_i direction of arrival;

$\mathbf{A} = [\mathbf{a}(\theta_1) \ \mathbf{a}(\theta_2) \ \cdots \ \mathbf{a}(\theta_N)]$ $M \times N$ matrix of steering vector $\mathbf{a}(\theta_i)$.

In a communication channel, noise is an undesired random signal, often modelled as additive white gaussian noise (AWGN), that may be caused by thermal noise or electromagnetic interference (EMI) from unknown sources. Noise should not be confused with crosstalk and other

interference from other communication system transmitters. Another possible source of the communication channel noise is the reflection from the ground when the antenna elements are close to the ground surface. Similarly, the reflection from antenna tower supporting the array antenna can be another source of noise. The effect of the reflection from antenna tower may be more serious if the antenna tower is electrically conducting.

III. NEWTON METHOD

Newton method make a sequence $\theta^{(i)}$ from an initial guess $\theta^{(0)}$ that converges towards $\theta^{(\text{true})}$ such that $P'(\theta^{(\text{true})}) = 0$ [27]. This $\theta^{(\text{true})}$ corresponds to one of the estimates of true AOA's. The second order Taylor expansion $P_T(\theta)$ of function $P(\theta)$ around $\theta^{(i)}$ is

$$P_T(\theta^{(i)} + \Delta\theta) = P(\theta^{(i)}) + P'(\theta^{(i)})\Delta\theta + \frac{1}{2}P''(\theta^{(i)})(\Delta\theta)^2, \quad (2)$$

which attains its extrema when its derivative with respect to $\Delta\theta$ is equal to zero,

$$P'(\theta^{(i)}) + P''(\theta^{(i)})(\Delta\theta) = 0. \quad (3)$$

Thus, provided that $P(\theta)$ is a twice-differentiable function well approximated by its second order Taylor expansion and the initial guess $\theta^{(0)}$ is chosen close enough to $\theta^{(\text{true})}$, the sequence $\theta^{(i)}$ defined by the following sequence will converge to $\theta^{(\text{true})}$,

$$\theta^{(i+1)} = \theta^{(i)} - \frac{P'(\theta^{(i)})}{P''(\theta^{(i)})} \quad i = 0, 1, \dots \quad (4)$$

IV. CONVENTIONAL BEAM FORMING ALGORITHM

In the conventional beam forming algorithm for AOA estimation, the array output power is computed as the arrival angle varies, and the arrival angles corresponding to the local maxima value in the output power distribution are considered to be the estimates of the true directions of arrival. AOA's are selected from the angle at which the following output achieves the local maxima,

$$P_{\text{CBF}}(\theta) = \mathbf{a}^H(\theta)\hat{\mathbf{R}}\mathbf{a}(\theta) \quad (5)$$

where θ is the arrival angle of an interest, and $\hat{\mathbf{R}}$

is the ML (maximum likelihood) estimate of the array output covariance matrix \mathbf{R} . That is, we evaluate equation (5) as a function of θ at discrete values, and find θ 's at which $P_{\text{CBF}}(\theta)$ achieve the local maxima.

We consider the case that there are N incident signals. We compute the beam forming spectrum at,

$$\left\{ \begin{array}{l} \theta_{\text{start}}, \theta_{\text{start}} + \Delta\theta, \theta_{\text{start}} + 2\Delta\theta, \dots, \theta_{\text{start}} \\ + \left\lfloor \frac{\theta_{\text{stop}} - \theta_{\text{start}}}{\Delta\theta} \right\rfloor \Delta\theta \end{array} \right\}. \quad (6)$$

The initial angle estimates, $\theta_1^{(0)}, \theta_2^{(0)}, \dots, \theta_N^{(0)}$, are found from the N local maxima of $\mathbf{a}^H(\theta) \hat{\mathbf{R}} \mathbf{a}(\theta)$ out of all the $P_{\text{CBF}}(\theta)$ in equation (5) at the following discrete angles,

$$\theta = \theta_{\text{start}}, \theta_{\text{start}} + \Delta\theta, \theta_{\text{start}} + 2\Delta\theta, \dots, \theta_{\text{start}} + \left\lfloor \frac{\theta_{\text{stop}} - \theta_{\text{start}}}{\Delta\theta} \right\rfloor \Delta\theta \quad (7)$$

where $\lfloor \cdot \rfloor$ rounds the argument toward zero. θ_{start} and θ_{stop} specify a search range of the angle, and $\Delta\theta$ is a search step.

Consider the case of the ULA and the UCA with M antenna elements. The array manifold is expressed as follows [1],

$$\mathbf{a}(\theta) = [\exp(j\psi_1) \exp(j\psi_2) \dots \exp(j\psi_M)]^T. \quad (8)$$

A. ULA

The symbol ψ_m for the ULA is given by,

$$\psi_m = (m-1) \frac{2\pi}{\lambda} d \sin \theta \quad m = 1, \dots, M. \quad (9)$$

If the distance between the antenna elements in the ULA is $\lambda/2$, equation (9) can be written as,

$$\psi_m = (m-1)\pi \sin \theta \quad m = 1, \dots, M. \quad (10)$$

Using equations (8) and (10) in equation (5), after some manipulation, for the ULA, we have,

$$\begin{aligned} P_{\text{CBF}}(\theta) &= \mathbf{a}^H(\theta) \hat{\mathbf{R}} \mathbf{a}(\theta) \\ &= \begin{bmatrix} e^{-j\psi_1} & \dots & e^{-j\psi_M} \end{bmatrix} \begin{bmatrix} \hat{R}_{11} & \dots & \hat{R}_{1M} \\ \vdots & \ddots & \vdots \\ \hat{R}_{M1} & \dots & \hat{R}_{MM} \end{bmatrix} \\ &= \begin{bmatrix} \sum_{m=1}^M e^{-j\psi_m} \hat{R}_{m1} & \dots & \sum_{m=1}^M e^{-j\psi_m} \hat{R}_{mM} \end{bmatrix} \begin{bmatrix} e^{j\psi_1} \\ \vdots \\ e^{j\psi_M} \end{bmatrix} \end{aligned}$$

$$\begin{aligned} P_{\text{CBF}}(\theta) &= \mathbf{a}^H(\theta) \hat{\mathbf{R}} \mathbf{a}(\theta) \\ &= \left(\sum_{m=1}^M e^{-j\psi_m} \hat{R}_{m1} \right) e^{j\psi_1} + \dots + \left(\sum_{m=1}^M e^{-j\psi_m} \hat{R}_{mM} \right) e^{j\psi_M} \\ &= \sum_{n=1}^M \sum_{m=1}^M e^{-j\psi_m} \hat{R}_{nm} e^{j\psi_n} = \sum_{n=1}^M \sum_{m=1}^M e^{j(\psi_n - \psi_m)} \hat{R}_{nm} \\ P_{\text{CBF, ULA}}(\theta) &= \sum_{m=1}^M \sum_{n=1}^M \exp[j(n-m)\pi \sin \theta] \hat{R}_{mn} \quad (11) \end{aligned}$$

where \hat{R}_{mn} denotes the m -th row and n -th column of the matrix $\hat{\mathbf{R}}$. Using equations (A3) and (A5) in appendix A, the following iteration is repeated until the update of the estimate is less than the specified tolerance [9]. That is, when the updates of all the estimates, $|\hat{\theta}_n^{(i+1)} - \hat{\theta}_n^{(i)}|$, $n = 1, \dots, N$, are less than the specified tolerance, the estimates are considered to be convergent,

$$\begin{aligned} \hat{\theta}_n^{(i+1)} &= \hat{\theta}_n^{(i)} - \frac{\frac{dP_{\text{CBF, ULA}}(\theta)}{d\theta}}{\frac{d}{d\theta} \left(\frac{dP_{\text{CBF, ULA}}(\theta)}{d\theta} \right)} \bigg|_{\theta=\hat{\theta}_n^{(i)}} \\ &= \hat{\theta}_n^{(i)} - \frac{\sum_{m=1}^M \sum_{n=1}^M [j(n-m)\pi \cos \hat{\theta}_n^{(i)}] \hat{R}_{mn} \exp(j(n-m)\pi \sin \hat{\theta}_n^{(i)})}{\sum_{m=1}^M \sum_{n=1}^M [j(n-m)\pi \exp(j(n-m)\pi \sin \hat{\theta}_n^{(i)}) (j(n-m)\pi \cos^2 \hat{\theta}_n^{(i)} - \sin \hat{\theta}_n^{(i)})] \hat{R}_{mn}} \\ & \quad i = 0, 1, \dots \quad n = 1, \dots, N. \quad (12) \end{aligned}$$

B. UCA

The symbol ψ_m for the UCA is written as,

$$\begin{aligned} \psi_m &= 2\pi \frac{r}{\lambda} \left[\cos \left(\theta - \frac{2\pi(m-1)}{M} \right) \right] \\ & \quad m = 1, \dots, M. \quad (13) \end{aligned}$$

Similarly, for the UCA, from equations (8), (13) and (5), we have,

$$\begin{aligned} P_{\text{CBF, UCA}}(\theta) &= \sum_{m=1}^M \sum_{n=1}^M \exp \left[-j4\pi \frac{r}{\lambda} \right. \\ & \quad \left. \sin \left(\theta - \frac{\pi(n+m-2)}{M} \right) \sin \left(\frac{\pi(m-n)}{M} \right) \right] \hat{R}_{mn}. \quad (14) \end{aligned}$$

For the UCA, using equations (A4) and (A6) in appendix A, we have,

$$\hat{\theta}_n^{(i+1)} = \hat{\theta}_n^{(i)} - \frac{\frac{dP_{\text{CBF, UCA}}(\theta)}{d\theta}}{\frac{d}{d\theta} \left(\frac{dP_{\text{CBF, UCA}}(\theta)}{d\theta} \right)} \Bigg|_{\theta=\hat{\theta}_n^{(i)}} \times \left[-j4\pi \frac{r}{\lambda} \sin \left(\frac{\pi(m-n)}{M} \right) \times \cos \left(\hat{\theta}_n^{(i)} - \frac{\pi(n+m-2)}{M} \right) \times \sum_{m=1}^M \sum_{n=1}^M \exp \left[-j4\pi \frac{r}{\lambda} \sin \left(\frac{\pi(m-n)}{M} \right) \times \sin \left(\hat{\theta}_n^{(i)} - \frac{\pi(n+m-2)}{M} \right) \right] \hat{R}_{mn} \right] \times \left[\sum_{m=1}^M \sum_{n=1}^M \exp \left[-j4\pi \frac{r}{\lambda} \sin \left(\frac{\pi(m-n)}{M} \right) \times \sin \left(\hat{\theta}_n^{(i)} - \frac{\pi(n+m-2)}{M} \right) \right] \times \left[j4\pi \frac{r}{\lambda} \sin \left(\frac{\pi(m-n)}{M} \right) \times \cos^2 \left(\hat{\theta}_n^{(i)} - \frac{\pi(n+m-2)}{M} \right) + \hat{R}_{mn} \right] \sin \left(\hat{\theta}_n^{(i)} - \frac{\pi(n+m-2)}{M} \right) \right] \hat{R}_{mn} \quad (15)$$

$i=0,1,\dots, n=1,\dots,N$

where $\hat{\theta}_n^{(i)}$ represents the AOA estimate for the i -th iteration of the n -th incident signal. The estimates obtained from the last iteration are designated as the final estimates, $\hat{\theta}_1^{(\text{final})}, \dots, \hat{\theta}_N^{(\text{final})}$. The termination criterion can be explicitly expressed as,

$$\left| \hat{\theta}_n^{(i+1)} - \hat{\theta}_n^{(i)} \right| < \text{tolerance} \quad n = 1, \dots, N. \quad (16)$$

The above iteration should be applied to each incident signals, respectively.

V. CAPON BEAM FORMING ALGORITHM

In the Capon beam forming algorithm for AOA estimation, AOA's are selected from the angles at which the following spectrum achieves the local maxima,

$$P_{\text{Capon}}(\theta) = \frac{1}{\mathbf{a}^H(\theta) \hat{\mathbf{R}}^{-1} \mathbf{a}(\theta)} \equiv \frac{1}{D_{\text{Capon}}(\theta)} \quad (17)$$

Where $D_{\text{Capon}}(\theta)$ is defined as follows,

$$D_{\text{Capon}}(\theta) = \mathbf{a}^H(\theta) \hat{\mathbf{R}}^{-1} \mathbf{a}(\theta). \quad (18)$$

The initial angle estimates, $\theta_1^{(0)}, \theta_2^{(0)}, \dots, \theta_N^{(0)}$, are found from the N local minima of $D_{\text{Capon}}(\theta) = \mathbf{a}^H(\theta) \hat{\mathbf{R}}^{-1} \mathbf{a}(\theta)$ at the discrete angles specified in equation (7). Note that, unlike the conventional beam forming algorithm, we have to find the angles, which are the local minima of $D_{\text{Capon}}(\theta) = \mathbf{a}^H(\theta) \hat{\mathbf{R}}^{-1} \mathbf{a}(\theta)$ because we have to maximize $P_{\text{Capon}}(\theta) = 1/D_{\text{Capon}}(\theta)$, which is equivalent to minimizing $D_{\text{Capon}}(\theta)$.

A. ULA

Using equations (10) and (8) in equation (18) results in,

$$D_{\text{Capon, ULA}}(\theta) = \sum_{m=1}^M \sum_{n=1}^M \exp[j(n-m)\pi \sin \theta] \hat{R}_{mn}^{-1}. \quad (19)$$

The iteration for the Capon beam forming can be explicitly written as,

$$\hat{\theta}_n^{(i+1)} = \hat{\theta}_n^{(i)} - \frac{\frac{dD_{\text{Capon, ULA}}(\theta)}{d\theta}}{\frac{d}{d\theta} \left(\frac{dD_{\text{Capon, ULA}}(\theta)}{d\theta} \right)} \Bigg|_{\theta=\hat{\theta}_n^{(i)}} \times \left[\sum_{m=1}^M \sum_{n=1}^M \left[j(n-m)\pi \cos \hat{\theta}_n^{(i)} \exp(j(n-m)\pi \sin \hat{\theta}_n^{(i)}) \right] \hat{R}_{mn}^{-1} \right] \times \left[\sum_{m=1}^M \sum_{n=1}^M \left[j(n-m)\pi \exp(j(n-m)\pi \sin \hat{\theta}_n^{(i)}) \left(j(n-m)\pi \cos^2 \hat{\theta}_n^{(i)} - \sin \hat{\theta}_n^{(i)} \right) \right] \hat{R}_{mn}^{-1} \right] \quad (20)$$

$i = 0, 1, \dots, n = 1, \dots, N.$

B. UCA

By substituting equations (8) and (13) in equation (18), we get, for the UCA,

$$D_{\text{Capon, UCA}}(\theta) = \sum_{m=1}^M \sum_{n=1}^M \exp \left[\begin{array}{c} -j4\pi \frac{r}{\lambda} \times \\ \sin \left(\theta - \frac{\pi(n+m-2)}{M} \right) \times \\ \sin \left(\frac{\pi(m-n)}{M} \right) \end{array} \right] \hat{R}_{mn}^{-1} \quad (21)$$

$$\hat{\theta}_n^{(i+1)} = \hat{\theta}_n^{(i)} - \frac{\frac{dD_{\text{Capon, UCA}}(\theta)}{d\theta}}{\frac{d}{d\theta} \left(\frac{dD_{\text{Capon, UCA}}(\theta)}{d\theta} \right)} \bigg|_{\theta=\hat{\theta}_n^{(i)}}$$

$$\hat{\theta}_n^{(i+1)} = \hat{\theta}_n^{(i)} - \frac{\sum_{m=1}^M \sum_{n=1}^M \left[\begin{array}{c} -j4\pi \frac{r}{\lambda} \sin \left(\frac{\pi(m-n)}{M} \right) \times \\ \cos \left(\hat{\theta}_n^{(i)} - \frac{\pi(n+m-2)}{M} \right) \end{array} \right] \exp \left[\begin{array}{c} -j4\pi \frac{r}{\lambda} \sin \left(\frac{\pi(m-n)}{M} \right) \times \\ \sin \left(\hat{\theta}_n^{(i)} - \frac{\pi(n+m-2)}{M} \right) \end{array} \right] \hat{R}_{mn}^{-1}}{j4\pi \frac{r}{\lambda} \sin \left(\frac{\pi(m-n)}{M} \right) \times \exp \left[\begin{array}{c} -j4\pi \frac{r}{\lambda} \sin \left(\frac{\pi(m-n)}{M} \right) \times \\ \sin \left(\hat{\theta}_n^{(i)} - \frac{\pi(n+m-2)}{M} \right) \end{array} \right] \sum_{m=1}^M \sum_{n=1}^M \left[\begin{array}{c} j4\pi \frac{r}{\lambda} \sin \left(\frac{\pi(m-n)}{M} \right) \times \\ \cos^2 \left(\hat{\theta}_n^{(i)} - \frac{\pi(n+m-2)}{M} \right) + \\ \sin \left(\hat{\theta}_n^{(i)} - \frac{\pi(n+m-2)}{M} \right) \end{array} \right] \hat{R}_{mn}^{-1}}$$

$$i=0,1,\dots, n=1,\dots,N, \quad (22)$$

where the termination criterion for the Capon algorithms is the same as that for the conventional beam forming algorithm.

VI. MUSIC ALGORITHM

The beam forming algorithm is the basic AOA algorithm, whose merit is the low computational cost [1, 22, 23]. In the beam forming algorithm, signals from certain directions are added constructively by forming a weighted sum of the array outputs. The antenna is steered to different directions by varying the array weights. On the other hand, in the MUSIC algorithm, we make use of the orthogonality between the noise eigenvectors and the array vectors corresponding to the true directions of incident signals in the MUSIC algorithm. In the MUSIC algorithm, the AOA's are obtained from the local maxima of the following spectrum,

$$P_{\text{MUSIC}}(\theta) = \frac{1}{\mathbf{a}^H(\theta) \mathbf{U}_N \mathbf{U}_N^H \mathbf{a}(\theta)} \equiv \frac{1}{D_{\text{MUSIC}}(\theta)} \quad (23)$$

where the columns of the matrix \mathbf{U}_N are the noise eigenvectors of the covariance matrix $\hat{\mathbf{R}}$, and $D_{\text{MUSIC}}(\theta)$ is defined as,

$$D_{\text{MUSIC}}(\theta) = \mathbf{a}^H(\theta) \mathbf{U}_N \mathbf{U}_N^H \mathbf{a}(\theta). \quad (24)$$

The array vector is defined in equations (8) and (10) for the ULA and equations (8) and (13) for the UCA. The initial estimates, $\theta_1^{(0)}$, $\theta_2^{(0)}$, ..., $\theta_N^{(0)}$, are obtained from the N local minima of $D_{\text{MUSIC}}(\theta)$ at the discrete angles specified in equation (7).

A. ULA

Substituting equations (10) and (8) in equation (24) yields,

$$D_{\text{MUSIC, ULA}}(\theta) = \sum_{m=1}^M \sum_{n=1}^M \exp [j(n-m)\pi \sin \theta] (\mathbf{U}_N \mathbf{U}_N^H)_{mn} \quad (25)$$

where $(\mathbf{U}_N \mathbf{U}_N^H)$ denotes the m -th row and the n -th column of the matrix $(\mathbf{U}_N \mathbf{U}_N^H)$. Using equations (C3) and (C5) in appendix C for the ULA, the following iterations are repeated until the convergence is achieved,

$$\hat{\theta}_n^{(i+1)} = \hat{\theta}_n^{(i)} - \frac{\frac{dD_{\text{MUSIC, ULA}}(\theta)}{d\theta}}{\frac{d}{d\theta} \left(\frac{dD_{\text{MUSIC, ULA}}(\theta)}{d\theta} \right)} \bigg|_{\theta=\hat{\theta}_n^{(i)}}$$

$$\hat{\theta}_n^{(i+1)} = \frac{\sum_{m=1}^M \sum_{n=1}^M \left[j(n-m)\pi \cos \hat{\theta}_n^{(i)} \times \exp \left(j(n-m)\pi \sin \hat{\theta}_n^{(i)} \right) \times (\mathbf{U}_N \mathbf{U}_N^H)_{mm} \right]}{j(n-m)\pi \exp \left(j(n-m)\pi \sin \hat{\theta}_n^{(i)} \right) \times \sum_{m=1}^M \sum_{n=1}^M \left(j(n-m)\pi \cos^2 \hat{\theta}_n^{(i)} - \sin \hat{\theta}_n^{(i)} \right) \times (\mathbf{U}_N \mathbf{U}_N^H)_{mm}}$$

$$i = 0, 1, \dots \quad n = 1, \dots, N \quad (26)$$

B. UCA

Similarly, from equations (13), (8) and (24), we have,

$$D_{\text{MUSIC, UCA}}(\theta) = \sum_{m=1}^M \sum_{n=1}^M \exp \left[-j4\pi \frac{r}{\lambda} \sin \left(\frac{\pi(m-n)}{M} \right) \times \sin \left(\theta - \frac{\pi(n+m-2)}{M} \right) \right] \times (\mathbf{U}_N \mathbf{U}_N^H)_{mm} \quad (27)$$

Using equations (B3) and (B5) from appendix B for the UCA, the following iterations are repeated until the convergence is achieved,

$$\hat{\theta}_n^{(i+1)} = \hat{\theta}_n^{(i)} - \frac{-j4\pi \frac{r}{\lambda} \sin \left(\frac{\pi(m-n)}{M} \right) \times \cos \left(\hat{\theta}_n^{(i)} - \frac{\pi(n+m-2)}{M} \right) \times \sum_{m=1}^M \sum_{n=1}^M \exp \left[-j4\pi \frac{r}{\lambda} \sin \left(\frac{\pi(m-n)}{M} \right) \times \sin \left(\hat{\theta}_n^{(i)} - \frac{\pi(n+m-2)}{M} \right) \right] \times (\mathbf{U}_N \mathbf{U}_N^H)_{mm}}{j4\pi \frac{r}{\lambda} \sin \left(\frac{\pi(m-n)}{M} \right) \times \exp \left[-j4\pi \frac{r}{\lambda} \sin \left(\frac{\pi(m-n)}{M} \right) \times \sin \left(\hat{\theta}_n^{(i)} - \frac{\pi(n+m-2)}{M} \right) \right] \times \sum_{m=1}^M \sum_{n=1}^M \left[j4\pi \frac{r}{\lambda} \sin \left(\frac{\pi(m-n)}{M} \right) \cos^2 \left(\hat{\theta}_n^{(i)} - \frac{\pi(n+m-2)}{M} \right) + \sin \left(\hat{\theta}_n^{(i)} - \frac{\pi(n+m-2)}{M} \right) \right] \times (\mathbf{U}_N \mathbf{U}_N^H)_{mm}}$$

$$i=0, 1, \dots \quad n=1, \dots, N \quad (28)$$

We adopt the stopping criterion in equation (16) for the MUSIC algorithm.

VII. COMMENTS ON HOW TO GET THE INITIAL ESTIMATES

Similarly, in section IV, we use the conventional beam forming algorithm for getting the initial estimates, which will be refined by applying the Newton method to the conventional beam forming algorithm. The same is true for the Capon beam forming algorithm in section V. In section VI, we arbitrarily assume that the initial estimates, which will be refined by using the cost function of the MUSIC algorithm, are obtained from the MUSIC algorithm. That is, the same AOA algorithm is used for the initialization and the refinement of the estimates, which does not have to be necessarily true.

It is not necessarily true that the initial estimates, which will be subsequently refined via the Newton method applied to the cost function of the MUSIC algorithm, should be estimated by using the MUSIC algorithm. That is, we can use any AOA estimation algorithm for getting the initial estimates to be further refined by applying the Newton method to the cost function of the MUSIC algorithm. In addition, the alternating projection algorithm [26] is very popular algorithm for getting the initial estimates due to the fact that it is computationally efficient at the cost of an accuracy degradation of the initial estimates. Similarly, we can use any AOA estimation algorithm including the AP algorithm for getting the initial estimates, which will be refined by applying the Newton method to the cost function of the conventional beam forming algorithm, and the Capon beam forming algorithm.

VIII. NUMERICAL RESULTS

At first, we designate the computer specification and the Matlab environment. The computer specification is as follows: Intel® Pentium CPU G620 @ 2.60GHz (2 CPU) 3018MB RAM. The Matlab environment is as follows: Matlab version 7.11.0.584 (R2010b). The operating system: Microsoft windows XP version 5.1 (build 2600: service pack 3). Java VM version: Java 1.6.0_17-b04 with Sun microsystems Inc. Java HotSpot (TM) Client VM mixed mode. The version of the signal processing toolbox is version 6.14.

In this section, the validity of the proposed scheme is illustrated via numerical results. The ULA and the UCA are used and the number of antenna elements, M , is chosen to be five. $\theta^{(\text{start})}$ and $\theta^{(\text{stop})}$ are selected to be $\theta^{(\text{start})} = -80^\circ$ and $\theta^{(\text{stop})} = 80^\circ$. The distance between the antenna elements in the ULA is $\lambda/2$, and the radius of the UCA is 0.679λ . The number of snapshots used for the calculation of $\hat{\mathbf{R}}$ is chosen to be 64. The tolerance, which is the termination criterion for the iteration in equation (16) is 10^{-3} . The maximum number of iteration in the Newton method is 100. The RMSE (root mean square error) and operation time in Figs. 1–12 are obtained from the 1000 repetitions. The search steps, $\Delta\theta$, in equation (7) are chosen to be 1.2° , 4.7° , and 8.8° . The main beam width of the half-wavelength-spaced ULA consisting of M elements is $2\sin^{-1}(2/M)$. For $M = 5$, the beam width is $\text{BW} = 2\sin^{-1}(2/5) = 0.823$ (rad) = 47 (degrees). The two incident signals are chosen so that their separation is larger than the BW. The following is how we get the search steps used in the simulation, $(\text{BW}/4) \times [0.1 \ 0.4 \ 0.75] = [1.2^\circ \ 4.7^\circ \ 8.8^\circ]$. Note that $\text{BW}/4$ is a search step to get four samples in the main beam width. To make sure that we have more than four samples in the main beam width, the search step should be smaller than the $\text{BW}/4$. Therefore, we arbitrarily let the search steps be equal to 0.1 times $\text{BW}/4$, 0.4 times $\text{BW}/4$ and 0.75 times $\text{BW}/4$.

For $\Delta\theta = 1.2$, there are 40 sampled points within the main beam width. Similarly, the sampled points within the main beam width are 10 and 5 for $\Delta\theta = 4.7^\circ$ and $\Delta\theta = 8.8^\circ$, respectively. We investigate the RMSE (root mean square error) and the execution time for various true incident angles, the search steps and SNR's. We consider the case that there are two incident signals, which implies that N is equal to two. The results with legend 'CBF', 'CAPON', and 'MUSIC' refer to the initial estimates for the conventional beam forming, the Capon beam forming, and the MUSIC algorithm, respectively. The results with legend 'CBF+NT' refer to the estimates obtained by applying the Newton iteration to the initial estimates from the conventional beam forming algorithm. The results for the ULA are from equation (12), and those for the UCA are from equation (15).

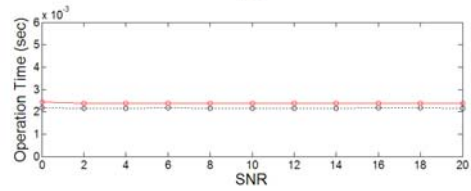
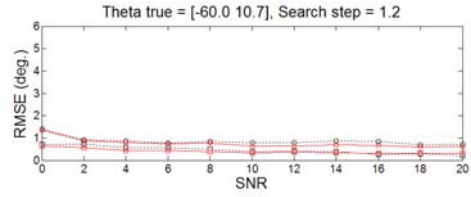
Similarly, the results with the legend 'CAPON+NT' refer to the final estimate obtained

by applying the Newton iteration to the initial estimates of the Capon beam forming algorithm. The results for the ULA are obtained from equation (20) and those for the UCA are obtained from equation (22). The Newton-iteration based final estimates for the MUSIC algorithm are shown with legend 'MUSIC+NT'. The results are from equations (26) and (28) for the ULA and the UCA, respectively. The results for the conventional beam forming are shown in Figs. 1, 4, 7, and 10, and those for the Capon beam forming are shown in Figs. 2, 5, 8, and 11. Figures 3, 6, 9, and 12 show the performance for the MUSIC algorithm. Figures 1–6 are for the ULA and Figs. 7–12 are for the UCA. Figures 1–3 show the performance improvement by the Newton iteration for a specific search step used for the calculation of the initial estimate for the conventional beam forming, the Capon beam forming, and the MUSIC algorithm, respectively. Figures 4–6 illustrate the fact that by employing the Newton iteration, we can improve the performance of the initial estimate obtained from the sparser search step. The results for the ULA with $[\theta_1^{(\text{true})} \ \theta_2^{(\text{true})}] = [-60^\circ \ -6.9^\circ]$ and $[\theta_1^{(\text{true})} \ \theta_2^{(\text{true})}] = [-60^\circ \ 10.7^\circ]$ and with the search steps, $\Delta\theta = 1.2^\circ$, $\Delta\theta = 4.7^\circ$, and $\Delta\theta = 8.8^\circ$ for various SNR's are shown in Figs. 1–3. The RMSE of the initial estimates and those of the final estimates are shown. The execution time is also illustrated to quantitatively describe the computational complexity of each scheme. The execution time of the algorithm is measured using Matlab function 'etime'.

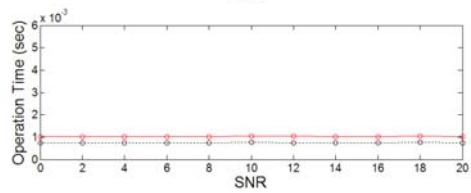
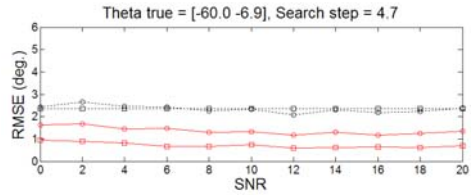
The final estimates are superior to the initial estimates in terms of the RMSE, but getting the final estimates take more time than getting the initial estimates, which can be seen in the second figure of each case because the final estimates are obtained by applying the Newton iteration to the initial estimates. The initial estimates in Figs. 1–3 for search step of 8.8° are inferior to those for search step of 4.7° because, in the case of $\Delta\theta = 8.8^\circ$, we use sparser grid points than in the case of $\Delta\theta = 4.7^\circ$ in estimating the initial estimates. Consequently, the execution time of the initial estimates for $\Delta\theta = 8.8^\circ$ is shorter than those for $\Delta\theta = 4.7^\circ$. From Figs. 1–3, we can see that the Newton iteration can improve the accuracy of the estimates at the expense of longer execution time. In Figs. 4–6, we show the results of the initial estimates

with the search step of $\Delta\theta = 1.2^\circ$ in equation (7) and those of the final estimates with $\Delta\theta = 4.7^\circ$. The performances of the initial estimates with $\Delta\theta = 1.2^\circ$ and those of the final estimates with $\Delta\theta = 4.7^\circ$ are approximately equal. But, it is clear from the figures that by applying the Newton iteration to the initial estimates obtained with $\Delta\theta = 4.7^\circ$, we can reduce the computational cost in comparison with the case that the initial estimates are obtained with $\Delta\theta = 1.2^\circ$ without applying the Newton iteration to the initial estimates.

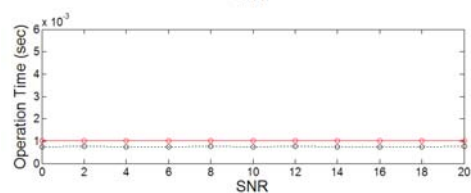
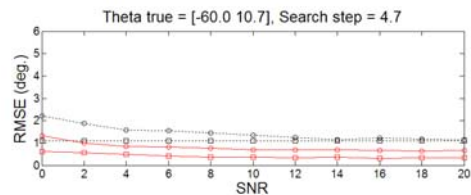
The difference between the results in Figs. 7–9 and those in Figs. 1–3 is the array structure employed for the implementation of the AOA estimation algorithm. The results in Figs. 7–9 are for the UCA, while those in Figs. 1–3 are for the ULA. For the same search step, getting the final estimates takes longer time than getting the initial estimates since the final estimates are obtained by applying the Newton iteration to the initial estimates. Figures 10–12 are for the UCA. The simulation conditions for the Figs. 10–12 are the same as those for the Figs. 4–6 except that Figs. 10–12 are for the UCA and that Figs. 4–6 are for the ULA.



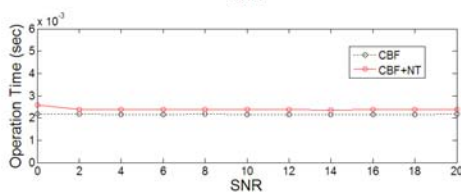
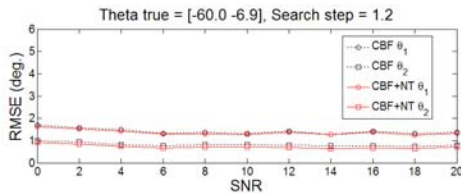
$$[\theta_1^{(\text{true})} \ \theta_2^{(\text{true})}] = [-60^\circ \ 10.7^\circ], \Delta\theta = 1.2^\circ$$



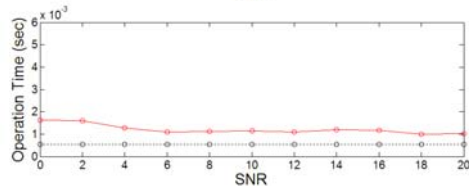
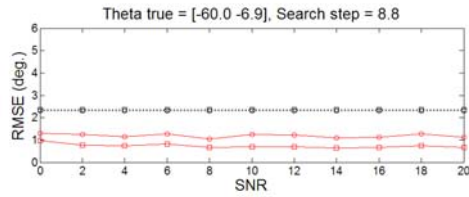
$$[\theta_1^{(\text{true})} \ \theta_2^{(\text{true})}] = [-60^\circ \ -6.9^\circ], \Delta\theta = 4.7^\circ$$



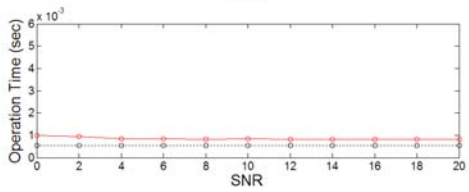
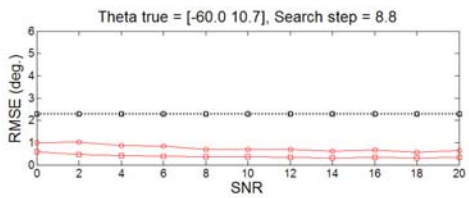
$$[\theta_1^{(\text{true})} \ \theta_2^{(\text{true})}] = [-60^\circ \ 10.7^\circ], \Delta\theta = 4.7^\circ$$



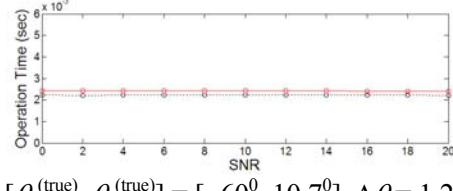
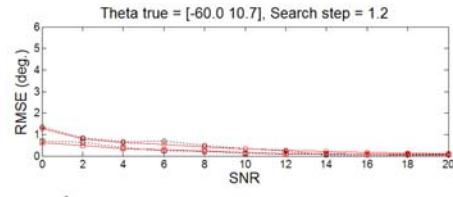
$$[\theta_1^{(\text{true})} \ \theta_2^{(\text{true})}] = [-60^\circ \ -6.9^\circ], \Delta\theta = 1.2^\circ$$



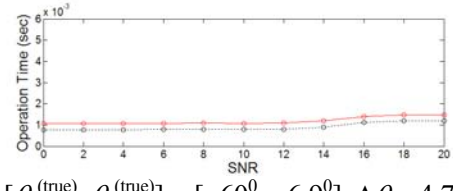
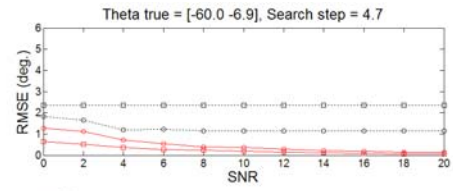
$$[\theta_1^{(\text{true})} \ \theta_2^{(\text{true})}] = [-60^0 \ -6.9^0], \Delta\theta = 8.8^0$$



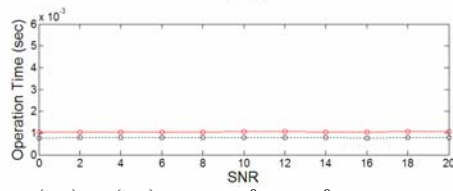
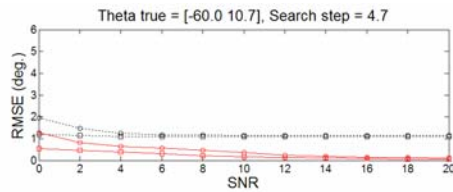
$$[\theta_1^{(\text{true})} \ \theta_2^{(\text{true})}] = [-60^0 \ 10.7^0], \Delta\theta = 8.8^0$$



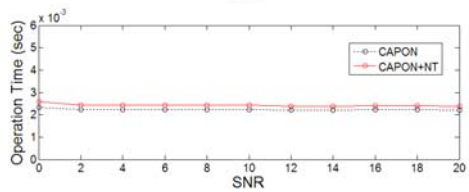
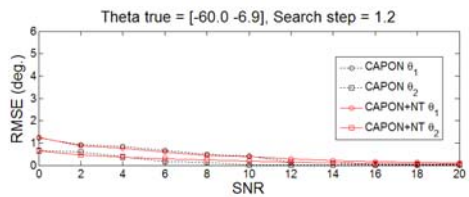
$$[\theta_1^{(\text{true})} \ \theta_2^{(\text{true})}] = [-60^0 \ 10.7^0], \Delta\theta = 1.2^0$$



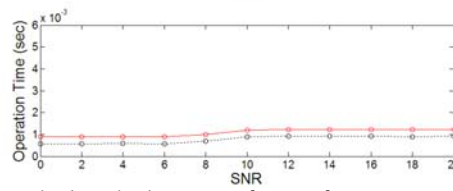
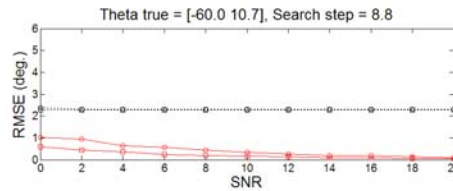
$$[\theta_1^{(\text{true})} \ \theta_2^{(\text{true})}] = [-60^0 \ -6.9^0], \Delta\theta = 4.7^0$$



$$[\theta_1^{(\text{true})} \ \theta_2^{(\text{true})}] = [-60^0 \ 10.7^0], \Delta\theta = 4.7^0$$

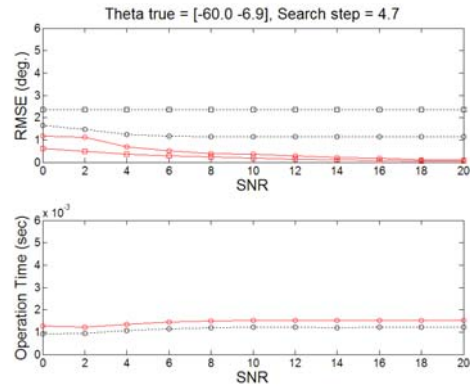
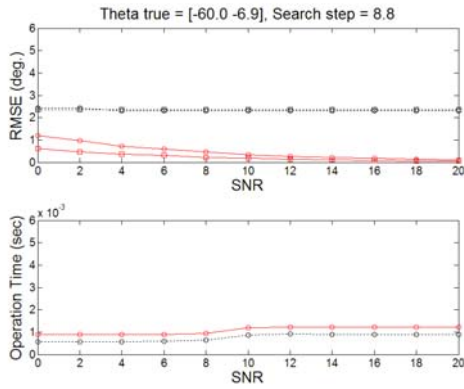


$$[\theta_1^{(\text{true})} \ \theta_2^{(\text{true})}] = [-60^0 \ -6.9^0], \Delta\theta = 1.2^0$$



$$[\theta_1^{(\text{true})} \ \theta_2^{(\text{true})}] = [-60^0 \ -6.9^0], \Delta\theta = 8.8^0$$

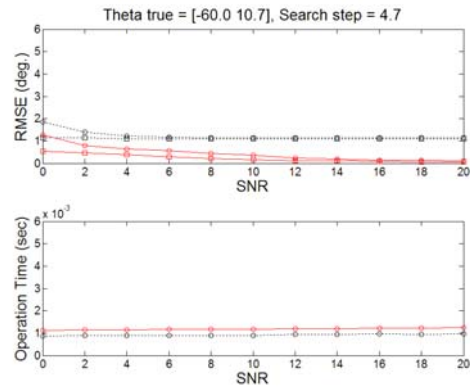
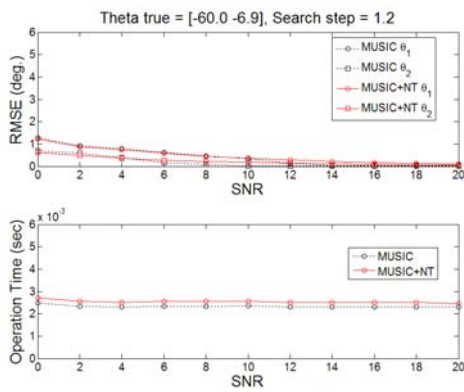
Fig. 1. Initial estimates without the Newton iteration and the final estimates with the Newton iteration of the conventional beam forming algorithm for the ULA.



$$[\theta_1^{(true)} \ \theta_2^{(true)}] = [-60^0 \ 10.7^0], \Delta\theta = 8.8^0$$

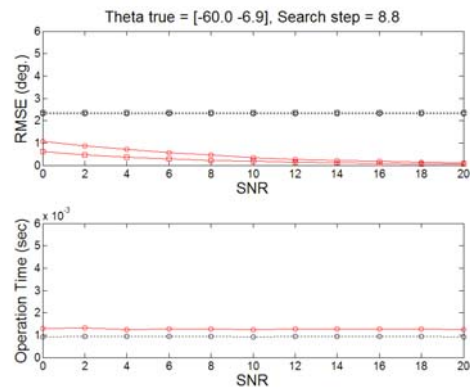
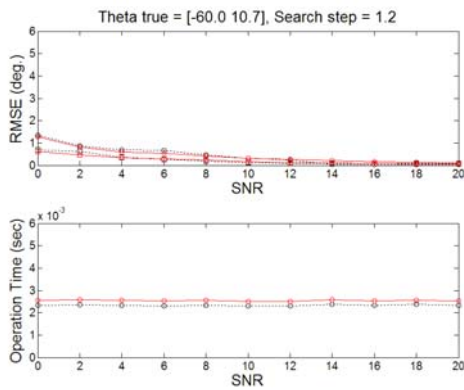
$$[\theta_1^{(true)} \ \theta_2^{(true)}] = [-60^0 \ -6.9^0], \Delta\theta = 4.7^0$$

Fig. 2. Initial estimates without the Newton iteration and the final estimates with the Newton iteration of the Capon beam forming algorithm for the ULA.



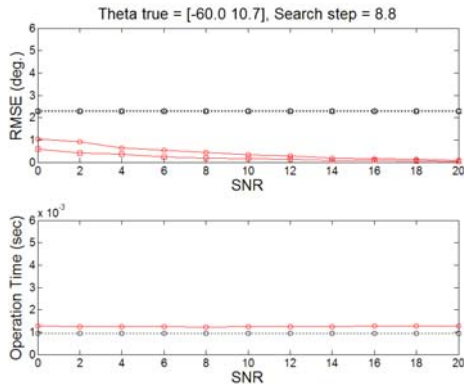
$$[\theta_1^{(true)} \ \theta_2^{(true)}] = [-60^0 \ -6.9^0], \Delta\theta = 1.2^0$$

$$[\theta_1^{(true)} \ \theta_2^{(true)}] = [-60^0 \ 10.7^0], \Delta\theta = 4.7^0$$



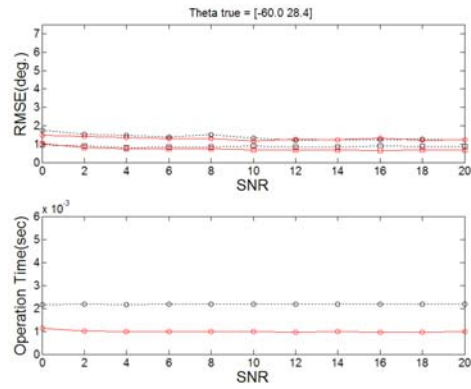
$$[\theta_1^{(true)} \ \theta_2^{(true)}] = [-60^0 \ 10.7^0], \Delta\theta = 1.2^0$$

$$[\theta_1^{(true)} \ \theta_2^{(true)}] = [-60^0 \ -6.9^0], \Delta\theta = 8.8^0$$

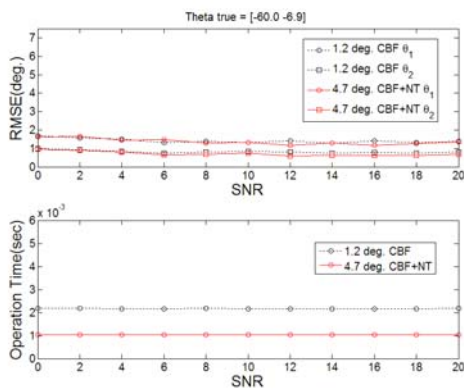


$$[\theta_1^{(\text{true})} \ \theta_2^{(\text{true})}] = [-60^0 \ 10.7^0], \Delta\theta = 8.8^0$$

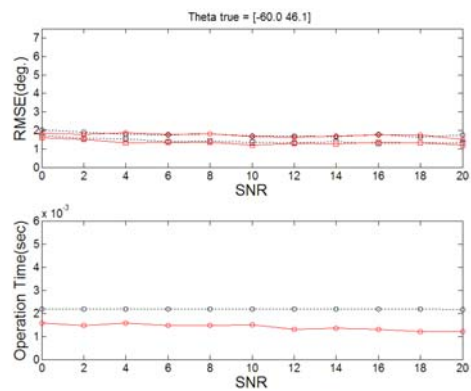
Fig. 3. Initial estimates without the Newton iteration and the final estimates with the Newton iteration of the MUSIC algorithm for the ULA.



$$[\theta_1^{(\text{true})} \ \theta_2^{(\text{true})}] = [-60^0 \ 28.4^0]$$

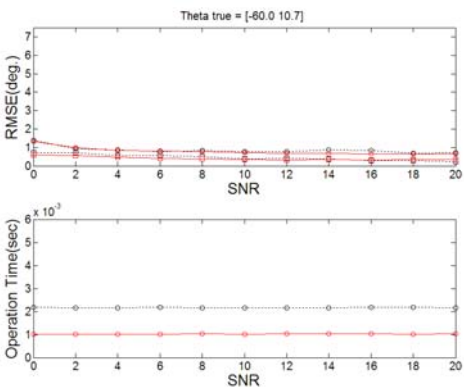


$$[\theta_1^{(\text{true})} \ \theta_2^{(\text{true})}] = [-60^0 \ -6.9^0]$$

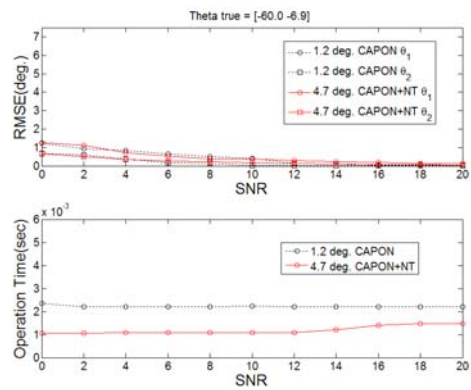


$$[\theta_1^{(\text{true})} \ \theta_2^{(\text{true})}] = [-60^0 \ 46.1^0]$$

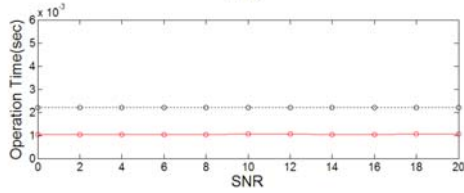
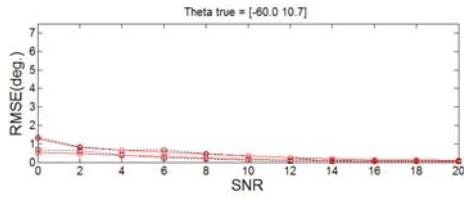
Fig. 4. Initial estimates for $\Delta\theta = 1.2^0$ without the Newton iteration and the final estimates for $\Delta\theta = 4.7^0$ with the Newton iteration of the conventional beam forming algorithm for the ULA.



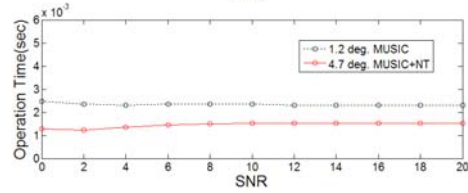
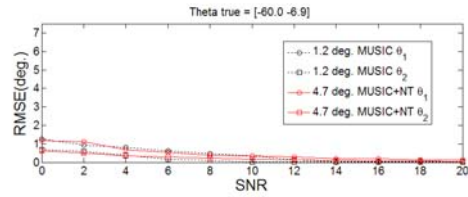
$$[\theta_1^{(\text{true})} \ \theta_2^{(\text{true})}] = [-60^0 \ 10.7^0]$$



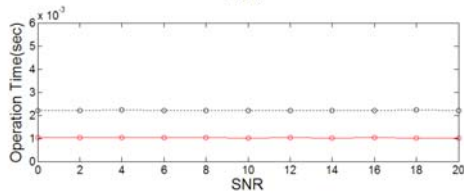
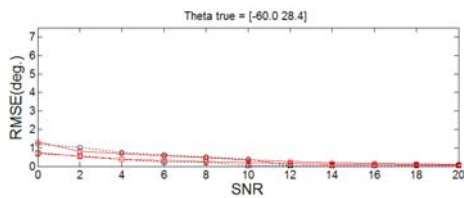
$$[\theta_1^{(\text{true})} \ \theta_2^{(\text{true})}] = [-60^0 \ -6.9^0]$$



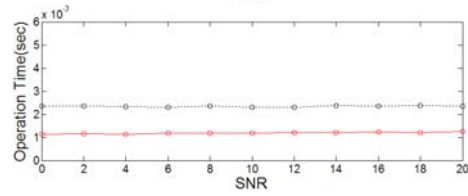
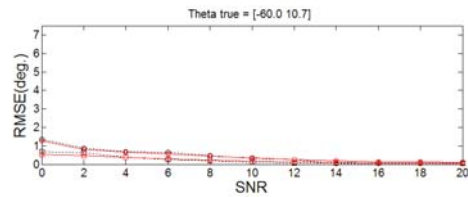
$$[\theta_1^{(\text{true})} \theta_2^{(\text{true})}] = [-60^0 \ 10.7^0]$$



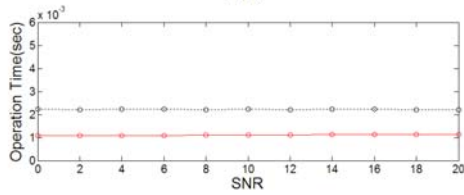
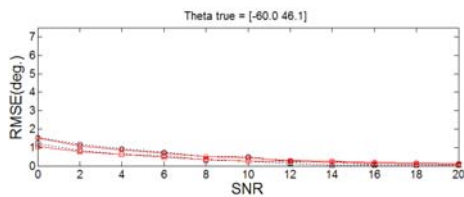
$$[\theta_1^{(\text{true})} \theta_2^{(\text{true})}] = [-60^0 \ -6.9^0]$$



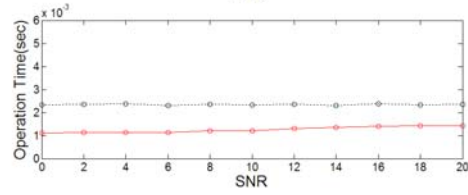
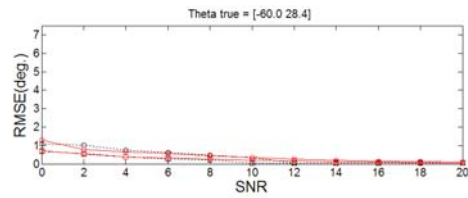
$$[\theta_1^{(\text{true})} \theta_2^{(\text{true})}] = [-60^0 \ 28.4^0]$$



$$[\theta_1^{(\text{true})} \theta_2^{(\text{true})}] = [-60^0 \ 10.7^0]$$

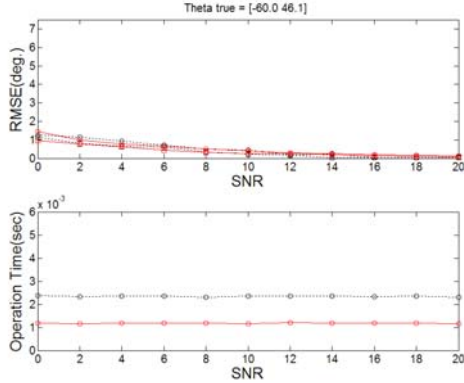


$$[\theta_1^{(\text{true})} \theta_2^{(\text{true})}] = [-60^0 \ 46.1^0]$$



$$[\theta_1^{(\text{true})} \theta_2^{(\text{true})}] = [-60^0 \ 28.4^0]$$

Fig. 5. Initial estimates for $\Delta\theta = 1.2^0$ without the Newton iteration and the final estimates for $\Delta\theta = 4.7^0$ with the Newton iteration of the Capon beam forming algorithm for the ULA.



$$[\theta_1^{(true)} \ \theta_2^{(true)}] = [-60^0 \ 46.1^0]$$

Fig. 6. Initial estimates for $\Delta\theta = 1.2^0$ without the Newton iteration and the final estimates for $\Delta\theta = 4.7^0$ with the Newton iteration of the MUSIC algorithm for the ULA.

Table 1: Quantitative improvement of the RMSE and the execution time in Figs. 1–3.

Conventional Beam forming		$[\theta_1^{(true)} \ \theta_2^{(true)}]$ $= [-60^\circ \ -6.9^\circ]$	$[\theta_1^{(true)} \ \theta_2^{(true)}]$ $= [-60^\circ \ 10.7^\circ]$		
Search step	True angle	RMSE improvement	Time increment	RMSE improvement	Time increment
1.2°	θ_1	3.4 %	10.8 %	11.2 %	10.2 %
	θ_2	12.0 %		9.9 %	
4.7°	θ_1	41.3 %	37.5 %	44.6 %	35.3 %
	θ_2	69.6 %		62.7 %	
8.8°	θ_1	48.6 %	123.4 %	67.3 %	56.9 %
	θ_2	69.0 %		83.0 %	

Capon Beam forming		$[\theta_1^{(true)} \ \theta_2^{(true)}]$ $= [-60^\circ \ -6.9^\circ]$	$[\theta_1^{(true)} \ \theta_2^{(true)}]$ $= [-60^\circ \ 10.7^\circ]$		
Search step	True angle	RMSE improvement	Time increment	RMSE improvement	Time increment
1.2°	θ_1	-5.3 %	9.0 %	-1.1 %	9.1 %
	θ_2	-32.9 %		2.5 %	
4.7°	θ_1	61.3 %	32.5 %	64.2 %	32.8 %
	θ_2	89.7 %		79.2 %	
8.8°	θ_1	79.6 %	41.3 %	81.0 %	39.5 %
	θ_2	89.9 %		90.3 %	

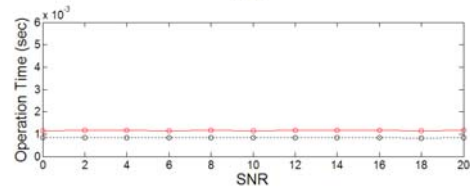
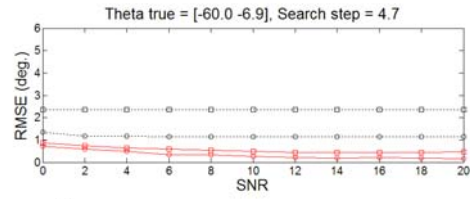
MUSIC		$[\theta_1^{(true)} \ \theta_2^{(true)}]$ $= [-60^\circ \ -6.9^\circ]$	$[\theta_1^{(true)} \ \theta_2^{(true)}]$ $= [-60^\circ \ 10.7^\circ]$		
Search step	True angle	RMSE improvement	Time increment	RMSE improvement	Time increment
1.2°	θ_1	-8.4 %	8.5 %	-1.3 %	8.7 %
	θ_2	-33.3 %		2.5 %	
4.7°	θ_1	61.6 %	26.7 %	63.9 %	28.6 %
	θ_2	89.8 %		79.4 %	
8.8°	θ_1	80.7 %	35.8 %	81.1 %	33.8 %
	θ_2	90.0 %		90.4 %	

Table 2: Quantitative improvement of the RMSE and the execution time in Figs. 4–6.

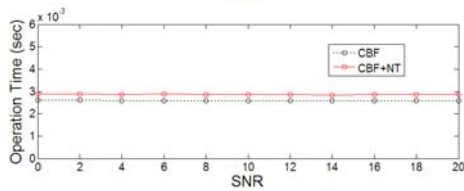
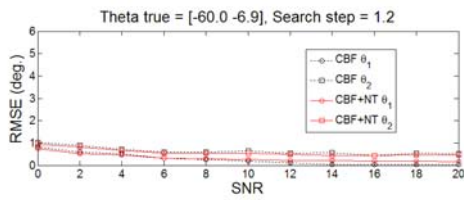
Conventional Beam forming				
True angle		Search step	1.2°, 4.7° +NT	
			θ_1	θ_2
$[\theta_1^{(true)} \ \theta_2^{(true)}]$ $= [-60^\circ \ -6.9^\circ]$	RMSE improvement	Time decrement	3.4 %	12.5 %
			52.1 %	
$[\theta_1^{(true)} \ \theta_2^{(true)}]$ $= [-60^\circ \ 10.7^\circ]$	RMSE improvement	Time decrement	7.0 %	10.1 %
			52.7 %	
$[\theta_1^{(true)} \ \theta_2^{(true)}]$ $= [-60^\circ \ 28.4^\circ]$	RMSE improvement	Time decrement	5.8 %	15.1 %
			54.1 %	
$[\theta_1^{(true)} \ \theta_2^{(true)}]$ $= [-60^\circ \ 46.1^\circ]$	RMSE improvement	Time decrement	2.0 %	5.6 %
			35.5 %	

Capon Beam forming				
True angle		Search step	1.2°, 4.7° +NT	
			θ_1	θ_2
$[\theta_1^{(true)} \ \theta_2^{(true)}]$ $= [-60^\circ \ -6.9^\circ]$	RMSE improvement	Time decrement	-8.3 %	-34.1 %
			46.5 %	
$[\theta_1^{(true)} \ \theta_2^{(true)}]$ $= [-60^\circ \ 10.7^\circ]$	RMSE improvement	Time decrement	-3.0 %	4.1 %
			52.6 %	
$[\theta_1^{(true)} \ \theta_2^{(true)}]$ $= [-60^\circ \ 28.4^\circ]$	RMSE improvement	Time decrement	-8.3 %	-21.7 %
			53.8 %	
$[\theta_1^{(true)} \ \theta_2^{(true)}]$ $= [-60^\circ \ 46.1^\circ]$	RMSE improvement	Time decrement	-2.7 %	-5.4 %
			50.2 %	

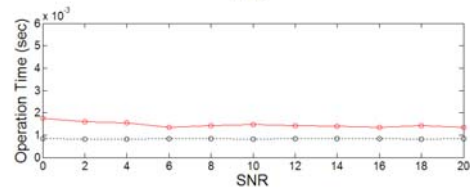
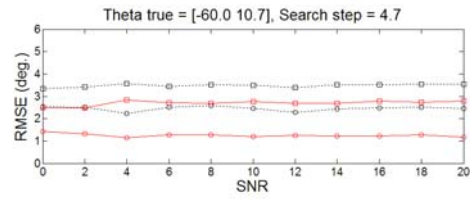
MUSIC			
True angle	Search step	1.2°, 4.7° +NT	
		θ_1	θ_2
$[\theta_1^{(true)} \quad \theta_2^{(true)}]$ $= [-60^\circ \quad -6.9^\circ]$	RMSE improvement	-9.1 %	-34.7 %
	Time decrement	37.9 %	
$[\theta_1^{(true)} \quad \theta_2^{(true)}]$ $= [-60^\circ \quad 10.7^\circ]$	RMSE improvement	-3.0 %	4.2 %
	Time decrement	49.3 %	
$[\theta_1^{(true)} \quad \theta_2^{(true)}]$ $= [-60^\circ \quad 28.4^\circ]$	RMSE improvement	-10.2 %	-16.1 %
	Time decrement	46.4 %	
$[\theta_1^{(true)} \quad \theta_2^{(true)}]$ $= [-60^\circ \quad 46.1^\circ]$	RMSE improvement	-4.1 %	-1.0 %
	Time decrement	49.8 %	



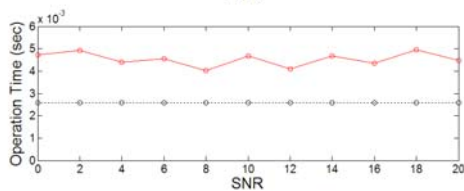
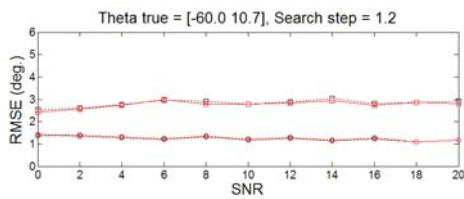
$$[\theta_1^{(true)} \quad \theta_2^{(true)}] = [-60^0 \quad -6.9^0], \Delta\theta = 4.7^0$$



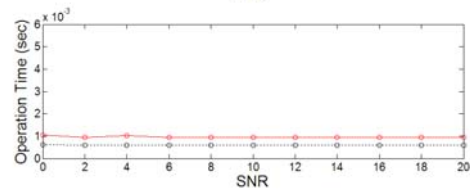
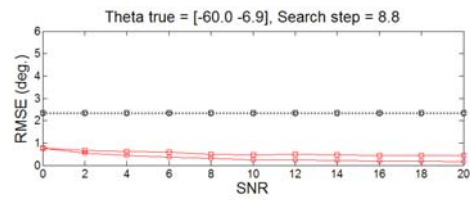
$$[\theta_1^{(true)} \quad \theta_2^{(true)}] = [-60^0 \quad -6.9^0], \Delta\theta = 1.2^0$$



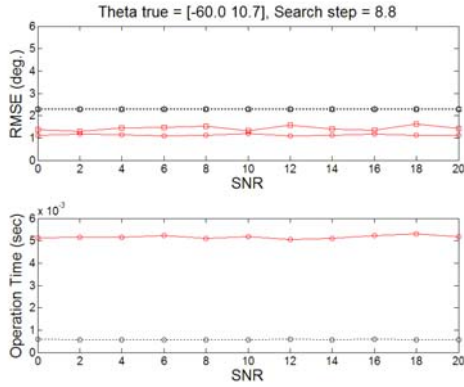
$$[\theta_1^{(true)} \quad \theta_2^{(true)}] = [-60^0 \quad 10.7^0], \Delta\theta = 4.7^0$$



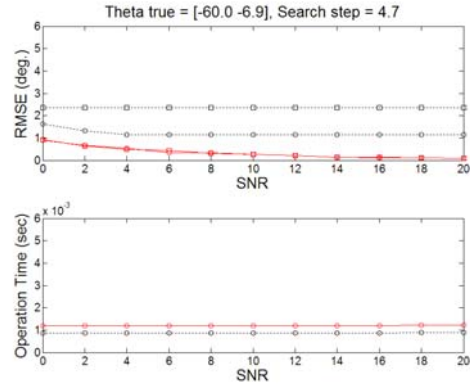
$$[\theta_1^{(true)} \quad \theta_2^{(true)}] = [-60^0 \quad 10.7^0], \Delta\theta = 1.2^0$$



$$[\theta_1^{(true)} \quad \theta_2^{(true)}] = [-60^0 \quad -6.9^0], \Delta\theta = 8.8^0$$

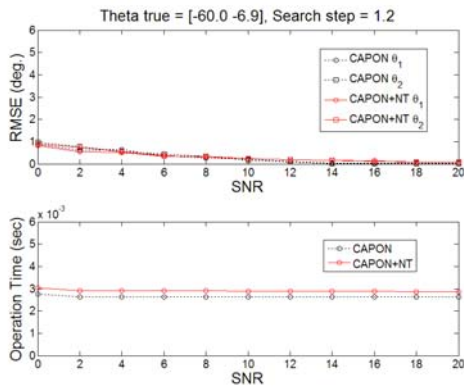


$$[\theta_1^{(\text{true})} \theta_2^{(\text{true})}] = [-60^0 \ 10.7^0], \Delta\theta = 8.8^0$$

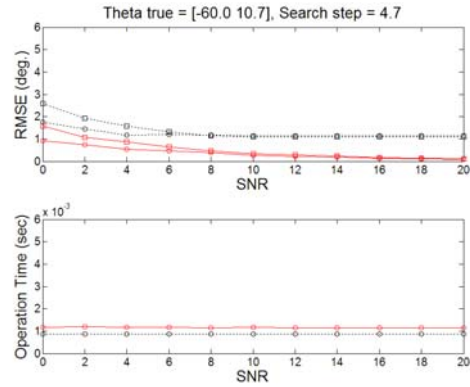


$$[\theta_1^{(\text{true})} \theta_2^{(\text{true})}] = [-60^0 \ -6.9^0], \Delta\theta = 4.7^0$$

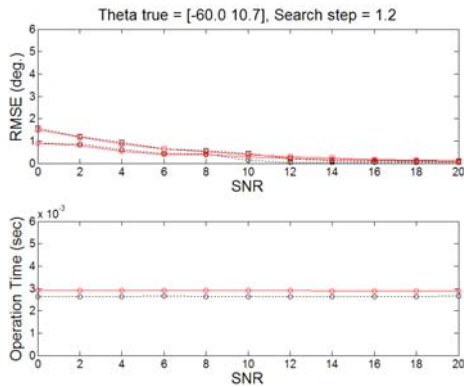
Fig. 7. Initial estimates without the Newton iteration and the final estimates with the Newton iteration of the conventional beam forming algorithm for the UCA.



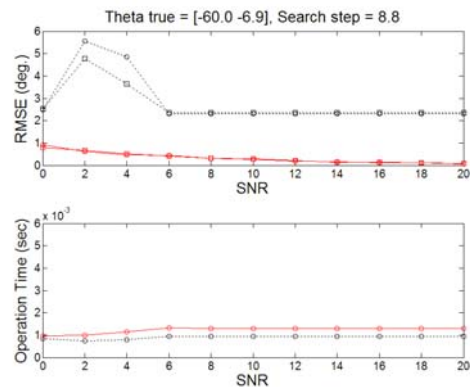
$$[\theta_1^{(\text{true})} \theta_2^{(\text{true})}] = [-60^0 \ -6.9^0], \Delta\theta = 1.2^0$$



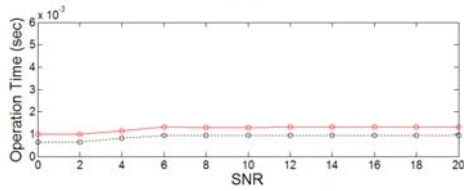
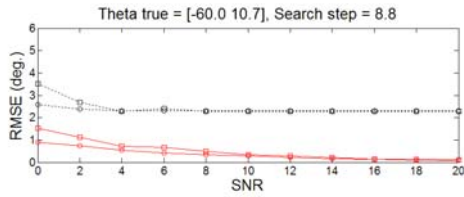
$$[\theta_1^{(\text{true})} \theta_2^{(\text{true})}] = [-60^0 \ 10.7^0], \Delta\theta = 4.7^0$$



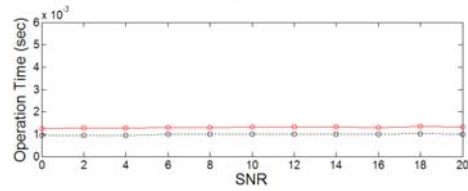
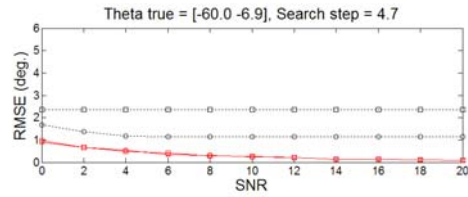
$$[\theta_1^{(\text{true})} \theta_2^{(\text{true})}] = [-60^0 \ 10.7^0], \Delta\theta = 1.2^0$$



$$[\theta_1^{(\text{true})} \theta_2^{(\text{true})}] = [-60^0 \ -6.9^0], \Delta\theta = 8.8^0$$

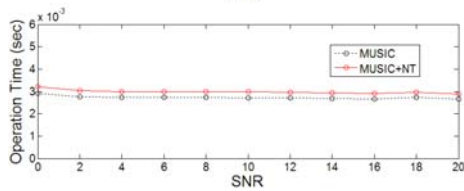
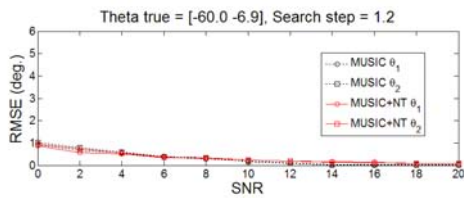


$$[\theta_1^{(true)} \ \theta_2^{(true)}] = [-60^0 \ 10.7^0], \Delta\theta = 8.8^0$$

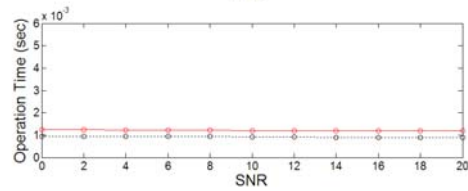
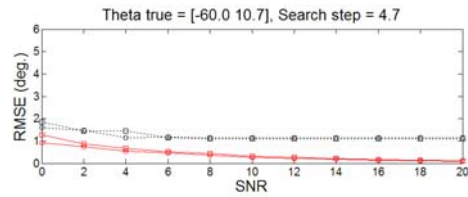


$$[\theta_1^{(true)} \ \theta_2^{(true)}] = [-60^0 \ -6.9^0], \Delta\theta = 4.7^0$$

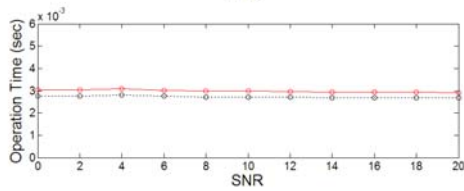
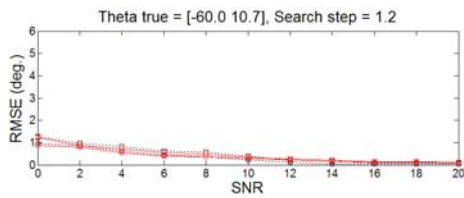
Fig. 8. Initial estimates without the Newton iteration and the final estimates with the Newton iteration of the Capon beam forming algorithm for the UCA.



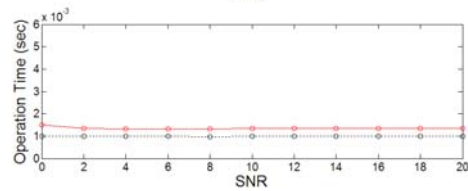
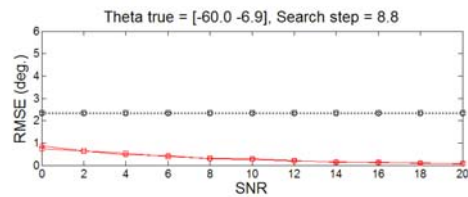
$$[\theta_1^{(true)} \ \theta_2^{(true)}] = [-60^0 \ -6.9^0], \Delta\theta = 1.2^0$$



$$[\theta_1^{(true)} \ \theta_2^{(true)}] = [-60^0 \ 10.7^0], \Delta\theta = 4.7^0$$



$$[\theta_1^{(true)} \ \theta_2^{(true)}] = [-60^0 \ 10.7^0], \Delta\theta = 1.2^0$$



$$[\theta_1^{(true)} \ \theta_2^{(true)}] = [-60^0 \ -6.9^0], \Delta\theta = 8.8^0$$

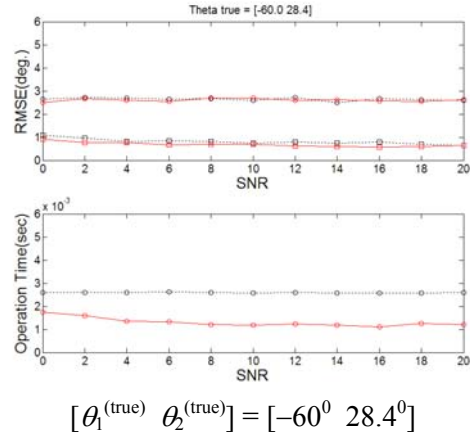
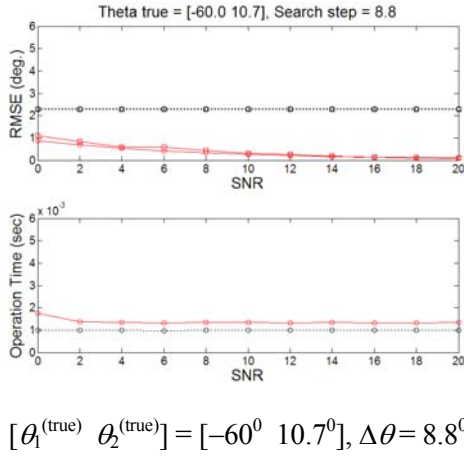


Fig. 9. Initial estimates without the Newton iteration and the final estimates with the Newton iteration of the MUSIC algorithm for the UCA.

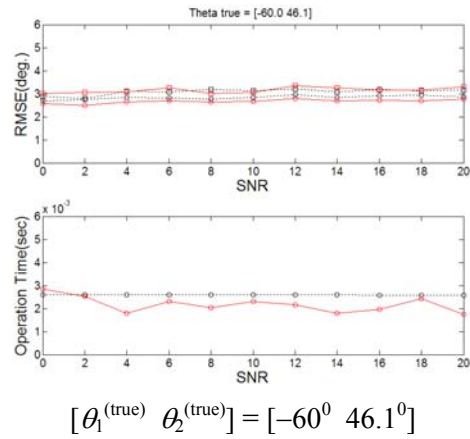
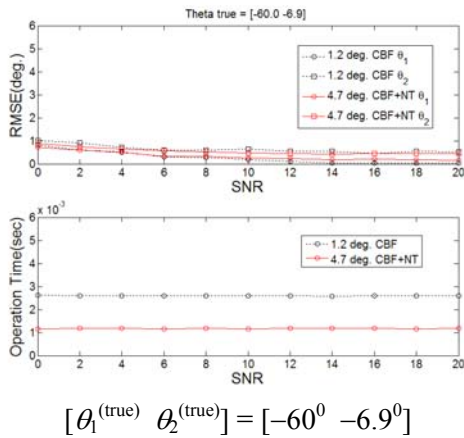
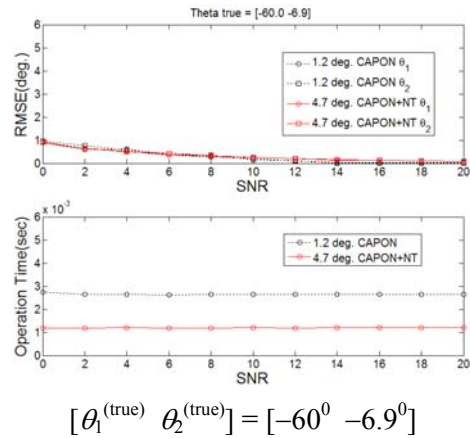
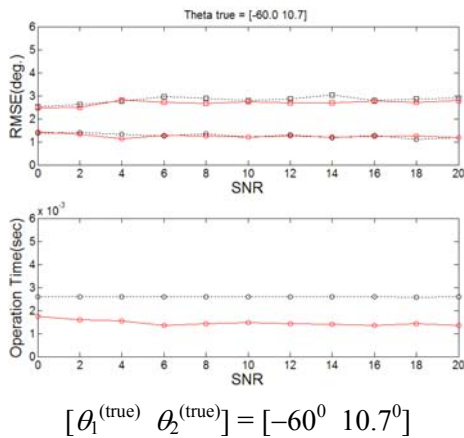
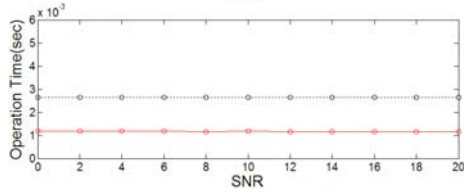
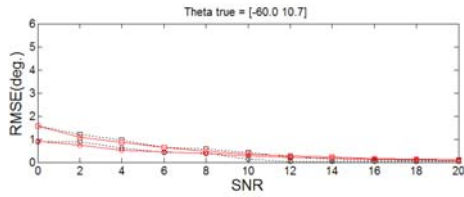
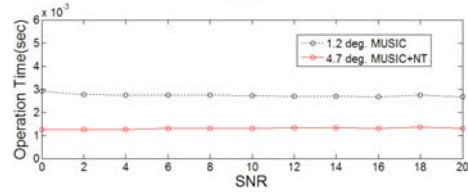
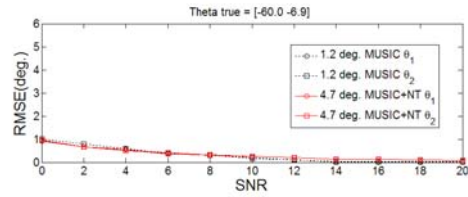


Fig. 10. Initial estimates for $\Delta\theta = 1.2^0$ without the Newton iteration and the final estimates for $\Delta\theta = 4.7^0$ with the Newton iteration of the conventional beam forming algorithm for the UCA.

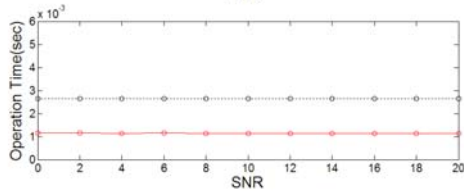
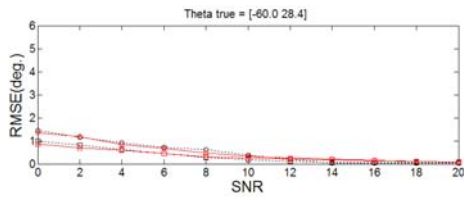




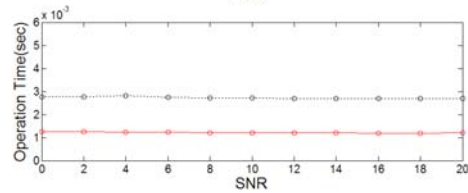
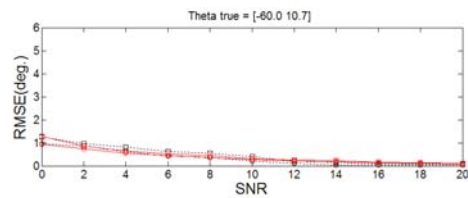
$$[\theta_1^{(\text{true})} \ \theta_2^{(\text{true})}] = [-60^0 \ 10.7^0]$$



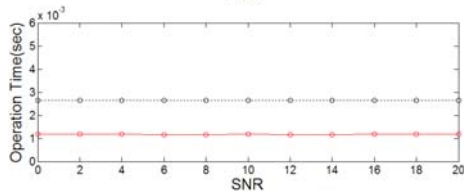
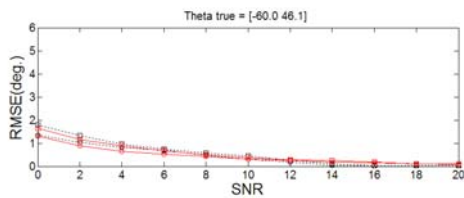
$$[\theta_1^{(\text{true})} \ \theta_2^{(\text{true})}] = [-60^0 \ -6.9^0]$$



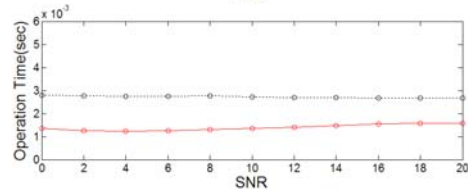
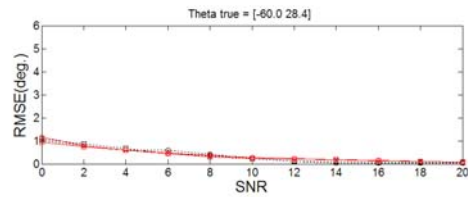
$$[\theta_1^{(\text{true})} \ \theta_2^{(\text{true})}] = [-60^0 \ 28.4^0]$$



$$[\theta_1^{(\text{true})} \ \theta_2^{(\text{true})}] = [-60^0 \ 10.7^0]$$

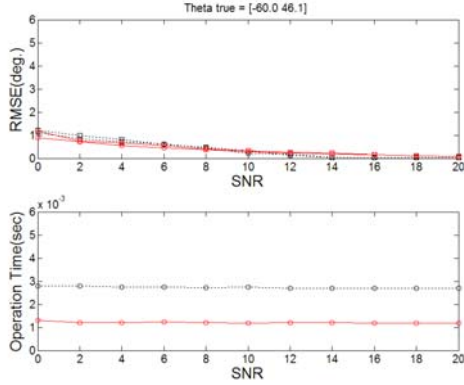


$$[\theta_1^{(\text{true})} \ \theta_2^{(\text{true})}] = [-60^0 \ 46.1^0]$$



$$[\theta_1^{(\text{true})} \ \theta_2^{(\text{true})}] = [-60^0 \ 28.4^0]$$

Fig. 11. Initial estimates for $\Delta\theta = 1.2^0$ without the Newton iteration and the final estimates for $\Delta\theta = 4.7^0$ with the Newton iteration of the Capon beam forming algorithm for the UCA.



$$[\theta_1^{(true)} \ \theta_2^{(true)}] = [-60^0 \ 46.1^0]$$

Fig. 12. Initial estimates for $\Delta\theta = 1.2^0$ without the Newton iteration and the final estimates for $\Delta\theta = 4.7^0$ with the Newton iteration of the MUSIC algorithm for the UCA.

Table 3: Quantitative improvement of the RMSE and the execution time in Figs. 7–9.

Conventional Beam forming		$[\theta_1^{(true)} \ \theta_2^{(true)}]$ $= [-60^\circ \ -6.9^\circ]$		$[\theta_1^{(true)} \ \theta_2^{(true)}]$ $= [-60^\circ \ 10.7^\circ]$	
Search step	True angle	RMSE improvement	Time increment	RMSE improvement	Time increment
1.2°	θ_1	-20.6 %	10.3 %	2.5 %	74.7 %
	θ_2	11.0 %		1.9 %	
4.7°	θ_1	71.0 %	38.5 %	48.9 %	74.9 %
	θ_2	76.4 %		22.6 %	
8.8°	θ_1	85.5 %	60.4 %	51.0 %	78.7 %
	θ_2	77.5 %		36.9 %	

Capon Beam forming		$[\theta_1^{(true)} \ \theta_2^{(true)}]$ $= [-60^\circ \ -6.9^\circ]$		$[\theta_1^{(true)} \ \theta_2^{(true)}]$ $= [-60^\circ \ 10.7^\circ]$	
Search step	True angle	RMSE improvement	Time increment	RMSE improvement	Time increment
1.2°	θ_1	-8.2 %	9.5 %	-10.9 %	9.7 %
	θ_2	-10.5 %		-0.8 %	
4.7°	θ_1	72.1 %	36.6 %	70.1 %	33.1 %
	θ_2	85.5 %		61.0 %	
8.8°	θ_1	88.3 %	34.6 %	84.9 %	40.6 %
	θ_2	87.8 %		78.4 %	

MUSIC		$[\theta_1^{(true)} \ \theta_2^{(true)}]$ $= [-60^\circ \ -6.9^\circ]$		$[\theta_1^{(true)} \ \theta_2^{(true)}]$ $= [-60^\circ \ 10.7^\circ]$	
Search step	True angle	RMSE improvement	Time increment	RMSE improvement	Time increment
1.2°	θ_1	-6.0 %	9.2 %	-5.3 %	9.3 %
	θ_2	-11.2 %		2.7 %	
4.7°	θ_1	72.3 %	32.6 %	69.8 %	31.1 %
	θ_2	85.3 %		63.4 %	
8.8°	θ_1	85.7 %	37.7 %	85.0 %	40.1 %
	θ_2	86.3 %		81.1 %	

Table 4: Quantitative improvement of the RMSE and the execution time in Figs. 10–12.

Conventional Beam forming			
True angle	Search step	1.2°, 4.7° +NT	
		θ_1	θ_2
$[\theta_1^{(true)} \ \theta_2^{(true)}]$ $= [-60^\circ \ -6.9^\circ]$	RMSE improvement	-25.4 %	14.1 %
	Time decrement	55.1 %	
$[\theta_1^{(true)} \ \theta_2^{(true)}]$ $= [-60^\circ \ 10.7^\circ]$	RMSE improvement	1.2 %	4.6 %
	Time decrement	43.5 %	
$[\theta_1^{(true)} \ \theta_2^{(true)}]$ $= [-60^\circ \ 28.4^\circ]$	RMSE improvement	1.5 %	15.3 %
	Time decrement	49.4 %	
$[\theta_1^{(true)} \ \theta_2^{(true)}]$ $= [-60^\circ \ 46.1^\circ]$	RMSE improvement	6.0 %	-2.2 %
	Time decrement	16.3 %	

Capon Beam forming			
True angle	Search step	1.2°, 4.7° +NT	
		θ_1	θ_2
$[\theta_1^{(true)} \ \theta_2^{(true)}]$ $= [-60^\circ \ -6.9^\circ]$	RMSE improvement	-14.1 %	-10.5 %
	Time decrement	54.7 %	
$[\theta_1^{(true)} \ \theta_2^{(true)}]$ $= [-60^\circ \ 10.7^\circ]$	RMSE improvement	-12.8 %	0.8 %
	Time decrement	56.0 %	
$[\theta_1^{(true)} \ \theta_2^{(true)}]$ $= [-60^\circ \ 28.4^\circ]$	RMSE improvement	0.1 %	-5.4 %
	Time decrement	56.7 %	
$[\theta_1^{(true)} \ \theta_2^{(true)}]$ $= [-60^\circ \ 46.1^\circ]$	RMSE improvement	1.8 %	2.4 %
	Time decrement	55.9 %	

MUSIC				
True angle		Search step	1.2°, 4.7° +NT	
			θ_1	θ_2
$[\theta_1^{(true)} \quad \theta_2^{(true)}]$		RMSE improvement	-11.6 %	-11.7 %
$= [-60^\circ \quad -6.9^\circ]$			Time decrement	
$[\theta_1^{(true)} \quad \theta_2^{(true)}]$		RMSE improvement	-7.9 %	4.7 %
$= [-60^\circ \quad 10.7^\circ]$			Time decrement	
$[\theta_1^{(true)} \quad \theta_2^{(true)}]$		RMSE improvement	-12.7 %	1.5 %
$= [-60^\circ \quad 28.4^\circ]$			Time decrement	
$[\theta_1^{(true)} \quad \theta_2^{(true)}]$		RMSE improvement	5.9 %	-0.4 %
$= [-60^\circ \quad 46.1^\circ]$			Time decrement	

It is clearly shown that the performance of the final estimates for $\Delta\theta = 4.7^\circ$ with the Newton iteration is nearly as good as the that of the initial estimates for $\Delta\theta = 1.2^\circ$ without the Newton iteration for all the three algorithms and that the computational complexity of getting the final estimates for $\Delta\theta = 4.7^\circ$ is less than that of getting the initial estimates for $\Delta\theta = 1.2^\circ$. In Tables 1–4, we clearly indicate quantitative improvement of the proposed method over the conventional method, which does not employ the Newton iteration in Figs. 1–12. The improvement of the RMSE and the execution time is indicated.

IX. CONCLUSION

In this paper, we propose essentially different approach of applying the Newton iteration to the AOA estimate to improve the accuracy of the AOA estimate. We apply the Newton iteration to the initial estimate obtained from the beam forming algorithm and the MUSIC algorithm to obtain the final estimates, which are more accurate than the initial estimates. We have demonstrated the performance improvement using the numerical results.

It is quite straightforward to apply the proposed scheme to other AOA estimation algorithm. In this paper, we showed the results for the case that there are two incident signals. It is also possible to apply the proposed scheme when there are more than two incident signals because the Newton iteration is applied to each incident signal, respectively. The scheme can also be applied to any arbitrary array structure by modifying the array vector consistently. The improvement of the proposed method over the

conventional method in terms of the RMSE and the execution time is shown in Tables 1–4, qualitatively.

APPENDIX A

To find the angles, which are the local maxima of equation (11), we find the angle at which the derivative of equation (11) is zero. If we differentiate equation (11) with respect to θ , we have,

$$\frac{dP_{\text{CBF,ULA}}(\theta)}{d\theta} = \sum_{m=1}^M \sum_{n=1}^M j(n-m)\pi \cos \theta \exp(j(n-m)\pi \sin \theta) \hat{R}_{mn}. \quad (\text{A1})$$

For the UCA, differentiating equation (14) with respect to θ yields,

$$\begin{aligned} & \frac{dP_{\text{CBF,UCA}}(\theta)}{d\theta} \\ &= \sum_{m=1}^M \sum_{n=1}^M \left[-j4\pi \frac{r}{\lambda} \sin\left(\frac{\pi(m-n)}{M}\right) \cos\left(\theta - \frac{\pi(n+m-2)}{M}\right) \right] \\ & \quad \exp\left[-j4\pi \frac{r}{\lambda} \sin\left(\frac{\pi(m-n)}{M}\right) \sin\left(\theta - \frac{\pi(n+m-2)}{M}\right)\right] \hat{R}_{mn}. \end{aligned} \quad (\text{A2})$$

Since equation (A1) is the derivative of equation (11), to find the angles which are local maxima of equation (11), we have to find the solution of,

$$\begin{aligned} & \frac{dP_{\text{CBF,ULA}}(\theta)}{d\theta} \\ &= \sum_{m=1}^M \sum_{n=1}^M j(n-m)\pi \cos \theta \exp(j(n-m)\pi \sin \theta) \hat{R}_{mn} = 0. \end{aligned} \quad (\text{A3})$$

Similarly, to find the local maxima of equation (14), we have to find the solution of the following,

$$\begin{aligned} & \frac{dP_{\text{CBF,UCA}}(\theta)}{d\theta} = \sum_{m=1}^M \sum_{n=1}^M \left\{ -j4\pi \frac{r}{\lambda} \sin\left(\frac{\pi(m-n)}{M}\right) \cos\left(\theta - \frac{\pi(n+m-2)}{M}\right) \right\} \\ & \quad \exp\left[-j4\pi \frac{r}{\lambda} \sin\left(\frac{\pi(m-n)}{M}\right) \sin\left(\theta - \frac{\pi(n+m-2)}{M}\right)\right] \hat{R}_{mn} = 0. \end{aligned} \quad (\text{A4})$$

Since the local maxima of equation (11) are obtained from the solutions of equation (A3), the initial guess of the solution of equation (A3) are the initial AOA estimates of equation (11). As previously stated, the initial guesses of the solution of equation (A3) are also calculated from the N local maxima of $\mathbf{a}^H(\theta) \hat{\mathbf{R}} \mathbf{a}(\theta)$ at the discrete angles given by equation (7). $\mathbf{a}(\theta)$ are defined in equations (8) and (10). Similarly, the initial estimates of equation (A4), which is for the UCA, are calculated from the N local maxima of $\mathbf{a}^H(\theta) \hat{\mathbf{R}} \mathbf{a}(\theta)$ at the discrete angles given by equation (7) and $\mathbf{a}(\theta)$ is defined in equations (8) and (13).

Our concern is, given the initial estimates, $\theta_1^{(0)}$, $\theta_2^{(0)}, \dots, \theta_N^{(0)}$, how to find the solutions of equations (A3) and (A4) numerically. The final estimates, $\theta_1^{(\text{final})}$, $\theta_2^{(\text{final})}, \dots, \theta_N^{(\text{final})}$, can be found using the iterative update. To find the solutions of equation (A3) using the Newton iteration, we have to find the derivative of $[dP_{\text{CBF,ULA}}(\theta)/d\theta]$ and $[dP_{\text{CBF,UCA}}(\theta)/d\theta]$ with respect to θ . The derivative of equation (A3) is easily obtained to be,

$$\begin{aligned} \frac{d}{d\theta} \left(\frac{dP_{\text{CBF,ULA}}(\theta)}{d\theta} \right) &= \sum_{m=1}^M \sum_{n=1}^M \left[-j(n-m)\pi \sin \theta \right. \\ &\quad \left. + (j(n-m)\pi)^2 \cos^2 \theta \right] \hat{R}_{mn}^{-1} \\ &= \sum_{m=1}^M \sum_{n=1}^M \left(j(n-m)\pi \cos^2 \theta - \sin \theta \right) \hat{R}_{mn}^{-1} \end{aligned} \quad (\text{A5})$$

Similarly, the derivative of (A4) is,

$$\begin{aligned} \frac{d}{d\theta} \left(\frac{dP_{\text{CBF,UCA}}(\theta)}{d\theta} \right) &= \sum_{m=1}^M \sum_{n=1}^M \left[j4\pi \frac{r}{\lambda} \sin \left(\frac{\pi(m-n)}{M} \right) \sin \left(\theta - \frac{\pi(n+m-2)}{M} \right) \right. \\ &\quad \left. \exp \left[-j4\pi \frac{r}{\lambda} \sin \left(\frac{\pi(m-n)}{M} \right) \sin \left(\theta - \frac{\pi(n+m-2)}{M} \right) \right] \right. \\ &\quad \left. + \left(-j4\pi \frac{r}{\lambda} \sin \left(\frac{\pi(m-n)}{M} \right) \right)^2 \cos^2 \left(\theta - \frac{\pi(n+m-2)}{M} \right) \right. \\ &\quad \left. \exp \left[-j4\pi \frac{r}{\lambda} \sin \left(\frac{\pi(m-n)}{M} \right) \sin \left(\theta - \frac{\pi(n+m-2)}{M} \right) \right] \right] \hat{R}_{mn}^{-1} \\ &= \sum_{m=1}^M \sum_{n=1}^M \left[-j4\pi \frac{r}{\lambda} \sin \left(\frac{\pi(m-n)}{M} \right) \exp \left[\begin{aligned} & -j4\pi \frac{r}{\lambda} \sin \left(\frac{\pi(m-n)}{M} \right) \sin \left(\theta - \frac{\pi(n+m-2)}{M} \right) \\ & \sin \left(\theta - \frac{\pi(n+m-2)}{M} \right) \end{aligned} \right] \right. \\ &\quad \left. \begin{aligned} & \left[-j4\pi \frac{r}{\lambda} \sin \left(\frac{\pi(m-n)}{M} \right) \cos^2 \left(\theta - \frac{\pi(n+m-2)}{M} \right) \right. \\ & \left. - \sin \left(\theta - \frac{\pi(n+m-2)}{M} \right) \right] \hat{R}_{mn}^{-1} \end{aligned} \right] \end{aligned} \quad (\text{A6})$$

APPENDIX B

Differentiation of equations (19) and (21) with respect to θ gives,

$$\begin{aligned} \frac{dD_{\text{Capon,ULA}}(\theta)}{d\theta} &= \sum_{m=1}^M \sum_{n=1}^M j(n-m)\pi \cos \theta \exp(j(n-m)\pi \sin \theta) \hat{R}_{mn}^{-1} \end{aligned} \quad (\text{B1})$$

$$\begin{aligned} \frac{dD_{\text{Capon,UCA}}(\theta)}{d\theta} &= \left\{ \sum_{m=1}^M \sum_{n=1}^M -j4\pi \frac{r}{\lambda} \sin \left(\frac{\pi(m-n)}{M} \right) \cos \left(\theta - \frac{\pi(n+m-2)}{M} \right) \right. \\ &\quad \left. \exp \left[-j4\pi \frac{r}{\lambda} \sin \left(\frac{\pi(m-n)}{M} \right) \sin \left(\theta - \frac{\pi(n+m-2)}{M} \right) \right] \right\} \hat{R}_{mn}^{-1}. \end{aligned} \quad (\text{B2})$$

We have to find the solutions of,

$$\begin{aligned} \frac{dD_{\text{Capon,ULA}}(\theta)}{d\theta} &= \sum_{m=1}^M \sum_{n=1}^M j(n-m)\pi \cos \theta \exp(j(n-m)\pi \sin \theta) \hat{R}_{mn}^{-1} = 0 \end{aligned} \quad (\text{B3})$$

$$\begin{aligned} \frac{dD_{\text{Capon,UCA}}(\theta)}{d\theta} &= \left\{ \sum_{m=1}^M \sum_{n=1}^M -j4\pi \frac{r}{\lambda} \sin \left(\frac{\pi(m-n)}{M} \right) \cos \left(\theta - \frac{\pi(n+m-2)}{M} \right) \right. \\ &\quad \left. \exp \left[\begin{aligned} & -j4\pi \frac{r}{\lambda} \sin \left(\frac{\pi(m-n)}{M} \right) \sin \left(\theta - \frac{\pi(n+m-2)}{M} \right) \\ & \sin \left(\theta - \frac{\pi(n+m-2)}{M} \right) \end{aligned} \right] \right\} \hat{R}_{mn}^{-1} = 0. \end{aligned} \quad (\text{B4})$$

The derivatives of equations (B3) and (B4) are easily obtained to be,

$$\begin{aligned} \frac{d}{d\theta} \left(\frac{dD_{\text{Capon,ULA}}(\theta)}{d\theta} \right) &= \sum_{m=1}^M \sum_{n=1}^M \left[-j(n-m)\pi \sin \theta \right. \\ &\quad \left. + (j(n-m)\pi)^2 \cos^2 \theta \right] \hat{R}_{mn}^{-1} \\ &= \sum_{m=1}^M \sum_{n=1}^M \left(j(n-m)\pi \cos^2 \theta - \sin \theta \right) \hat{R}_{mn}^{-1} \end{aligned} \quad (\text{B5})$$

$$\begin{aligned} \frac{d}{d\theta} \left(\frac{dD_{\text{Capon,UCA}}(\theta)}{d\theta} \right) &= \sum_{m=1}^M \sum_{n=1}^M \left[j4\pi \frac{r}{\lambda} \sin \left(\frac{\pi(m-n)}{M} \right) \sin \left(\theta - \frac{\pi(n+m-2)}{M} \right) \right. \\ &\quad \left. \exp \left[-j4\pi \frac{r}{\lambda} \sin \left(\frac{\pi(m-n)}{M} \right) \sin \left(\theta - \frac{\pi(n+m-2)}{M} \right) \right] \right. \\ &\quad \left. + \left(-j4\pi \frac{r}{\lambda} \sin \left(\frac{\pi(m-n)}{M} \right) \right)^2 \cos^2 \left(\theta - \frac{\pi(n+m-2)}{M} \right) \right. \\ &\quad \left. \exp \left[-j4\pi \frac{r}{\lambda} \sin \left(\frac{\pi(m-n)}{M} \right) \sin \left(\theta - \frac{\pi(n+m-2)}{M} \right) \right] \right] \hat{R}_{mn}^{-1} \\ &= \sum_{m=1}^M \sum_{n=1}^M \left[-j4\pi \frac{r}{\lambda} \sin \left(\frac{\pi(m-n)}{M} \right) \exp \left[\begin{aligned} & -j4\pi \frac{r}{\lambda} \sin \left(\frac{\pi(m-n)}{M} \right) \sin \left(\theta - \frac{\pi(n+m-2)}{M} \right) \\ & \sin \left(\theta - \frac{\pi(n+m-2)}{M} \right) \end{aligned} \right] \right. \\ &\quad \left. \begin{aligned} & \left[-j4\pi \frac{r}{\lambda} \sin \left(\frac{\pi(m-n)}{M} \right) \cos^2 \left(\theta - \frac{\pi(n+m-2)}{M} \right) \right. \\ & \left. - \sin \left(\theta - \frac{\pi(n+m-2)}{M} \right) \right] \hat{R}_{mn}^{-1} \end{aligned} \right] \end{aligned} \quad (\text{B6})$$

APPENDIX C

The differentiation of equations (25) and (27) with respect to θ results in,

$$\frac{dD_{\text{MUSIC, ULA}}(\theta)}{d\theta} = \sum_{m=1}^M \sum_{n=1}^M j(n-m)\pi \cos \theta \exp(j(n-m)\pi \sin \theta) (\mathbf{U}_N \mathbf{U}_N^H)_{mn} \quad (\text{C1})$$

$$\begin{aligned} \frac{dD_{\text{MUSIC, UCA}}(\theta)}{d\theta} &= \sum_{m=1}^M \sum_{n=1}^M \left[\begin{array}{l} -j4\pi \frac{r}{\lambda} \sin\left(\frac{\pi(m-n)}{M}\right) \\ \cos\left(\theta - \frac{\pi(n+m-2)}{M}\right) \\ \exp\left[-j4\pi \frac{r}{\lambda} \sin\left(\frac{\pi(m-n)}{M}\right)\right] \\ \sin\left(\theta - \frac{\pi(n+m-2)}{M}\right) \end{array} \right] (\mathbf{U}_N \mathbf{U}_N^H)_{mn} \quad (\text{C2}) \end{aligned}$$

Accordingly, our objective is to find the solution of the followings,

$$\begin{aligned} \frac{dD_{\text{MUSIC, ULA}}(\theta)}{d\theta} &= \sum_{m=1}^M \sum_{n=1}^M j(n-m)\pi \cos \theta \exp(j(n-m)\pi \sin \theta) (\mathbf{U}_N \mathbf{U}_N^H)_{mn} \\ &= 0 \quad (\text{C3}) \end{aligned}$$

$$\begin{aligned} \frac{dD_{\text{MUSIC, UCA}}(\theta)}{d\theta} &= \sum_{m=1}^M \sum_{n=1}^M \left[\begin{array}{l} -j4\pi \frac{r}{\lambda} \sin\left(\frac{\pi(m-n)}{M}\right) \\ \cos\left(\theta - \frac{\pi(n+m-2)}{M}\right) \\ \exp\left[-j4\pi \frac{r}{\lambda} \sin\left(\frac{\pi(m-n)}{M}\right)\right] \\ \sin\left(\theta - \frac{\pi(n+m-2)}{M}\right) \end{array} \right] (\mathbf{U}_N \mathbf{U}_N^H)_{mn} = 0 \quad (\text{C4}) \end{aligned}$$

Differentiation of equation (C3) and (C4) results in,

$$\begin{aligned} \frac{d}{d\theta} \left(\frac{dD_{\text{MUSIC, ULA}}(\theta)}{d\theta} \right) &= \sum_{m=1}^M \sum_{n=1}^M \left[\begin{array}{l} -j(n-m)\pi \sin \theta \\ \exp(j(n-m)\pi \sin \theta) \\ + (j(n-m)\pi)^2 \cos^2 \theta \\ \exp(j(n-m)\pi \sin \theta) \end{array} \right] (\mathbf{U}_N \mathbf{U}_N^H)_{mn} \\ &= \sum_{m=1}^M \sum_{n=1}^M j(n-m)\pi \exp(j(n-m)\pi \sin \theta) (\mathbf{U}_N \mathbf{U}_N^H)_{mn} \\ &\quad - \sum_{m=1}^M \sum_{n=1}^M (j(n-m)\pi \cos^2 \theta - \sin \theta) (\mathbf{U}_N \mathbf{U}_N^H)_{mn} \quad (\text{C5}) \end{aligned}$$

$$\begin{aligned} \frac{d}{d\theta} \left(\frac{dD_{\text{MUSIC, UCA}}(\theta)}{d\theta} \right) &= \sum_{m=1}^M \sum_{n=1}^M \left[\begin{array}{l} j4\pi \frac{r}{\lambda} \sin\left(\frac{\pi(m-n)}{M}\right) \sin\left(\theta - \frac{\pi(n+m-2)}{M}\right) \\ \exp\left[-j4\pi \frac{r}{\lambda} \sin\left(\frac{\pi(m-n)}{M}\right)\right] \sin\left(\theta - \frac{\pi(n+m-2)}{M}\right) \\ + \left[-j4\pi \frac{r}{\lambda} \sin\left(\frac{\pi(m-n)}{M}\right)\right]^2 \cos^2\left(\theta - \frac{\pi(n+m-2)}{M}\right) \\ \exp\left[-j4\pi \frac{r}{\lambda} \sin\left(\frac{\pi(m-n)}{M}\right)\right] \cos^2\left(\theta - \frac{\pi(n+m-2)}{M}\right) \\ \exp\left[-j4\pi \frac{r}{\lambda} \sin\left(\frac{\pi(m-n)}{M}\right)\right] \sin\left(\theta - \frac{\pi(n+m-2)}{M}\right) \end{array} \right] (\mathbf{U}_N \mathbf{U}_N^H)_{mn} \\ &= \sum_{m=1}^M \sum_{n=1}^M \left[\begin{array}{l} -j4\pi \frac{r}{\lambda} \sin\left(\frac{\pi(m-n)}{M}\right) \exp\left[-j4\pi \frac{r}{\lambda} \sin\left(\frac{\pi(m-n)}{M}\right)\right] \\ \sin\left(\theta - \frac{\pi(n+m-2)}{M}\right) \\ \left[-j4\pi \frac{r}{\lambda} \sin\left(\frac{\pi(m-n)}{M}\right)\right]^2 \cos^2\left(\theta - \frac{\pi(n+m-2)}{M}\right) \\ - \sin\left(\theta - \frac{\pi(n+m-2)}{M}\right) \end{array} \right] (\mathbf{U}_N \mathbf{U}_N^H)_{mn} \quad (\text{C6}) \end{aligned}$$

ACKNOWLEDGMENT

This research was supported by Basic Science Research Program through the National Research Foundation of Korea (NRF) funded by the Ministry of Education, Science and Technology (2012-0002347).

REFERENCES

- [1] H. Krim and M. Viberg, "Two decades of array signal processing research – The parametric approach," *IEEE Signal Processing Magazine*, vol. 13, pp. 67-94, July 1996.
- [2] J. -H. Lee and S. -H. Cho, "On initialization of ML DOA cost function for UCA," *Progress in Electromagnetics Research M*, vol. 3, pp. 91-102, 2008.
- [3] J. -H. Lee, H. -J. Kwon, and Y. -K. Jin, "Numerically efficient implementation of JADE ML algorithm," *Journal of Electromagnetic Waves and Applications*, vol. 22, pp. 1693-1704, 2008.
- [4] J. -H. Lee and S. -H. Cho, "Initialization of cost function for ML-based DOA estimation," *The Journal of Korea Information and Communications Society*, vol. 33, no. 1, pp. 110-116, Jan. 2008.
- [5] M. Rubsamen and A. Gershman, "Direction-of-arrival estimation for non uniform sensor arrays: From manifold separation to Fourier domain MUSIC methods," *IEEE Trans. on Signal Processing*, vol. 57, no. 2, pp. 588-599, 2009.
- [6] S. A. Vorobyov, A. B. Gershman, and K. M. Wong, "Maximum likelihood direction-of-arrival

- estimation in unknown noise fields using sparse sensor arrays,” *IEEE Trans. Signal Processing*, vol. 53, pp. 34-43, Jan. 2005.
- [7] H. Cao, L. Yang, X. Tan, and S. Yang, “Computationally efficient 2-D DOA estimation using two parallel uniform linear arrays,” *ETRI Journal*, vol. 31, no. 6, pp. 806-808, Dec. 2009.
- [8] J. A. Olague, D. C. Rosales, and J. L. Rivera, “Efficiency evaluation of the unconditional maximum likelihood estimator for near-field DOA estimation,” *ETRI Journal*, vol. 28, no.6, pp. 761-769, Dec. 2006.
- [9] N. Deblauwe and L. Van Biesen, “An angle of arrival location estimation technique for existing GSM networks,” *IEEE International Conference on Signal Processing and Communications*, pp. 1527-1530, 2007.
- [10] S. Lalchand, A. Ijaz, M. M. Manzoor, I. A. Awan, and A. A. Siddique, “Error estimation in angle of arrival in smart antenna,” *International Conference on Information and Communication Technologies*, pp. 1-3, 2011.
- [11] I. Jami and R. F. Ormondroyd, “Improved method for estimating angle of arrival in multipath conditions using the ‘MUSIC’ algorithm,” *IEEE-APS Conference on Antennas and Propagation for Wireless Communications*, pp. 99-102, 2000.
- [12] I. Amundson, X. Koutsoukos, J. Sallai, and A. Ledeczki, “Mobile sensor navigation using rapid RF-based angle of arrival localization,” *17th IEEE Real-Time and Embedded Technology and Applications Symposium*, 2011.
- [13] Y. Luo and C. L. Law, “Angle-of-arrival estimation with array in a line-of-sight indoor UWB-IR,” *7th International Conference on Information, Communications and Signal Processing*, pp. 1-5, 2009.
- [14] J. Friedman, A. Davitian, D. Torres, D. Cabric, and M. Srivastava, “Angle-of-arrival-assisted relative interferometric localization using software defined radios,” *IEEE Military Communications Conference*, pp. 1-8, 2009.
- [15] V. Kezys, E. Vertatschitsch, T. Greenlay, and S. Haykin, “High-resolution techniques for angle-of-arrival estimation,” *IEEE Military Communications Conference - Communications-Computers: Teamed for the 90's*, pp. 41.3.1-41.3.6, 1986.
- [16] N. B. Buchanan and V. Fusco, “Angle of arrival detection using retrodirective radar,” *Radar Conference*, pp. 133-136, 2010.
- [17] T. Chan, Y. Kuga, and S. Roy, “Combined use of various passive radar techniques and angle of arrival using music for the detection of ground moving objects,” *IEEE International Symposium on Antennas and Propagation*, pp. 2561-2564, 2011.
- [18] J. Friedman, T. Schmid, Z. Charbiwala, M. B. Srivastava, and Y. H. Cho, “Multistatic pulse-wave angle-of-arrival-assisted relative interferometric radar,” *IEEE Radar Conference*, pp. 458- 463, 2011.
- [19] Y. Kalkan and B. Baykal, “Target localization and velocity estimation methods for frequency-only mimo radars,” *IEEE Radar Conference*, pp. 458-463, 2011.
- [20] Y. Norouzi and M. Derakhshani, “Joint time difference of arrival/angle of arrival position finding in passive radar,” *Radar, Sonar & Navigation, IET*, vol. 3, no.2, pp. 167-176, 2009.
- [21] C. Du, J. S. Thompson, and Y. R. Petillot, “Hybrid bistatic radar,” *International Radar Conference - Surveillance for a Safer World, International*, pp. 1-6, 2009.
- [22] J. Capon, “High resolution frequency-wavenumber spectrum analysis,” *Proceedings of the IEEE*, vol. 57, pp. 1408-1418, Aug. 1969.
- [23] J. -H. Lee, Y. S. Jeong, S. -W. Cho, W. Y. Yeo, and K. Pister, “Application of the Newton method to improve the accuracy of TOA estimation with the beam forming algorithm and the MUSIC algorithm,” *Progress in Electromagnetics Research*, vol. 116, pp. 475-515, 2011.
- [24] R. O. Schmidt, “Multiple emitter location and signal parameter estimation,” *Proceedings of RADC Spectral Est. Work shop*, pp. 243-258, Oct. 1979.
- [25] R. Roy, A. Paulraj, and T. Kailath, “ESPRIT – a subspace rotation approach to estimation of parameters of cisoids in noise,” *IEEE Trans. Acoustics, Speech, Signal Processing*, vol. 34, pp. 1340-1342, Oct. 1986.
- [26] I. Ziskind and M. Wax, “Maximum likelihood localization of multiple sources by alternating projection,” *IEEE Trans. on Signal Processing*, vol. 36, no. 10, pp. 1553-1560, Oct. 1988.
- [27] H. W. Press, P. B. Flannery, A. S. Teukolsky, and T. W. Vetterling, *Numerical Recipes in C*, Cambridge University Press, 1992.
- [28] http://en.wikipedia.org/wiki/Newton_method_in_optimization, August, 2012.



Joon-Ho Lee received the B.Sc. degree (Magna Cum Laude) in 1994, the M.Sc. degree in 1996, and the Ph.D. in 1999 in Electronics Engineering, all from Pohang University of Science and Technology (POSTECH), Pohang, Korea. From July 1999 to Feb.

2004, he was with Electronics and Telecommunications Research Institute (ETRI), Daejeon, Korea. Since March 2004, he has been with Sejong University, Seoul, Korea, where he is an Associate Professor with the Department of Information and Communication Eng. His research interests are in radio signal processing, array signal processing, spectrum estimation and radar target recognition. He was on Sabbatical leave at UC. Berkeley from Jan. 2010 to Jan. 2011.



Sung-Woo Cho received the B.Sc. degree in Information and Communication Engineering from Sejong University, Seoul, Korea in 2011. He is currently working toward his M.Sc. degree in Information and Communication Engineering from Sejong University.

His research interests include array signal processing and radio signal processing.